Animal Nutrition 21 (2025) 11–24

Contents lists available at ScienceDirect

Animal Nutrition

journal homepage: http://www.keaipublishing.com/en/journals/aninu/

Original Research Article

# Transcriptomics and non-targeted metabolomics provide mechanistic insights into the improvement of the growth performance and meat quality of lambs supplemented with fermented *Lycium barbarum* residues

Jiale Liao [a], Wencan Ke [a], Bing Wang [c], Min Du [d], Qiang Lu [a], Yajun Zhang [a], Guijie Zhang [a, b, *]

[a] College of Forestry and Prataculture, Ningxia University, Yinchuan 750021, China
[b] College of Animal Science and Technology, Ningxia University, Yinchuan 750021, China
[c] State Key Laboratory of Animal Nutrition, College of Animal Science and Technology, China Agricultural University, Beijing 100193, China
[d] Nutrigenomics and Growth Biology Laboratory, Department of Animal Sciences, Washington State University, Pullman, WA 99164, United States

ARTICLE INFO

*Article history:*
Received 23 November 2023
Received in revised form
2 November 2024
Accepted 13 November 2024
Available online 22 November 2024

*Keywords:*
Ruminant
Agro-industrial residue
Rumen fermentation
Meat quality
Lipid metabolism

ABSTRACT

This study investigated the effects of *Lycium barbarum* residues (LBR) and fermented *L. barbarum* residues (FLBR) on the growth performance and meat quality of lambs. Eighteen lambs were randomly assigned into three groups and fed either a basal diet (CON) or the same diet supplemented with 5.0% LBR or FLBR for a period of 90 days. The underlying mechanisms responsible for the beneficial effect of LBR and FLBR on the longissimus thoracis (LT) and intramuscular fat (IMF) tissues of lambs were examined using multiomics techniques. Our findings showed that FLBR supplementation significantly enhanced the average daily gain, feed efficiency, and nutrient digestibility ($P < 0.05$ or $P < 0.01$). Serum total protein ($P = 0.007$) and glucose ($P = 0.002$) levels were higher in the FLBR-fed lambs, while urea nitrogen level was lower ($P = 0.001$). Additionally, the levels of rumen acetate ($P = 0.002$) and propionate ($P = 0.011$) were significantly elevated, while ammonia-nitrogen ($NH_3$–N), isobutyrate and isovalerate decreased ($P < 0.05$ or $P < 0.01$) following FLBR supplementation. Post-mortem meat quality was also improved by FLBR, as evidenced by enhanced total antioxidant capacity, superoxide dismutase activity, pH, redness (a*), tenderness and water holding capacity ($P < 0.05$ or $P < 0.01$), alongside a reduction in the malonaldehyde content ($P < 0.001$). Transcriptomic analysis identified 962 differentially expressed genes (DEGs, FLBR vs CON) and 782 DEGs (FLBR vs LBR) in LT, and 1313 DEGs (FLBR vs CON) and 1221 DEGs (FLBR vs LBR) in IMF. The ribosome signaling pathway related genes in LT tissue were activated by the FLBR diet ($P < 0.05$), showing a higher anabolism of protein. The genes involved in fatty acid biosynthesis in IMF tissue were upregulated by the FLBR diet ($P < 0.05$), showing a higher anabolism of lipids. Metabolomics analysis identified the 1732 differential metabolites in LT tissue following FLBR supplementation, with significant alterations in metabolites such as carnosine, L-arginine and L-proline, which may serve as potential biomarkers for meat quality betterment. In conclusion, FLBR supplementation might have modified anabolism of proteins and fatty acid, as well as muscle metabolomic profiles, leading to improvements in both growth performance and meat quality in fattening lambs.


* Corresponding author.
*E-mail address:* guijiezhang@nxu.edu.cn (G. Zhang).
Peer review under the responsibility of Chinese Association of Animal Science and Veterinary Medicine.

Production and Hosting by Elsevier on behalf of KeAi

## 1. Introduction

As the demand of consumers for safer, healthier, and higher-quality meat rises, producers must quickly adopt more effective feed management practices. Tan lambs, a native breed from Ningxia Province, China, are highly valued for their high nutritive value,

https://doi.org/10.1016/j.aninu.2024.11.002

appealing flavor, and well-distributed fat (Gao et al., 2014). However, the rapid transition from grassland grazing to captive feeding with energy-dense diets has resulted in reduced levels of flavor-related compounds, poor meat tenderness, inconsistent color, and imbalanced fat distribution in lambs across China (Yang et al., 2024). The relatively lower feed efficiency and growth rates observed in ruminants, as opposed to monogastric animals, further limited the lamb production (Debi et al., 2022). Improving skeletal muscle development is essential for carcass muscle yield, while intramuscular fat (IMF) plays pivotal roles in meat juiciness, color and flavor (Long et al., 2022). The development of muscle and fat directly influences the growth performance of lambs. Therefore, there is an urgent need to explore optimal solutions for more efficient feed resources utilization to achieve commercial profitability and satisfy consumer preferences, thus facilitating the establishment of a sustainable fattening programming of lambs.

Breeders have modified diets with traditional Chinese herbs, such as *Radix astragali* and *Morinda officinalis*, to enhance the meat quality and productivity (Wang et al., 2017). However, the rapidly growing global population has precipitated a critical scarcity of these herbal resources, impeding their use in livestock production. Concerning the profitability and sustainability in the livestock production system, residues from these herbs could present a practical solution. *L. barbarum*, a valuable and medicinal shrub of the Solanaceae family, contains bioactive compounds like polysaccharides, carotenoids, polyphenols, betaine, and vitamins, which can confer immunomodulatory, antioxidant, anti-inflammatory, and disease-resistant benefits to domestic animals (Ma et al., 2022). Consequently, *L. barbarum* residues (LBR) may serve as a higher-quality feedstuff for livestock, offering distinct advantages over conventional diets. Despite its positive results in improving rabbit meat quality (Menchetti et al., 2020), and regulating lipid levels in hybrid groupers (Tan et al., 2019), scarce information is available on the functional roles of *L. barbarum* inclusion in the ruminant diets. The primary components of LBR included bits of leaves, pericarp, defective fruits and peduncles, which is typically regarded as a waste, thereby resulting in significant environmental pollution and economic loss. Therefore, it is crucial to process low-grade and agro-industrial residues into high-quality feed.

Numerous studies have demonstrated that the synergistic fermentation of agricultural by-products with beneficial microorganisms increases value as feed. For instance, soybean residues had significantly higher soluble proteins and total flavonoids following fermentation with *Bacillus subtilis* (Dai et al., 2017). Similarly, the chrysanthemum waste fermented with *Saccharomycetes* and *B. subtilis* showed elevated levels of soluble proteins, crude fat, calcium, phosphorus and flavonoids, along with a more balanced amino acid profile (Cui et al., 2023). Given these findings, the employment of probiotic-fermented feed has the potential to improve the growth, health, and product quality of ruminants. This study aimed to prepare a fermented LBR with probiotics, and evaluate its effects on the growth performance and post-mortem meat quality of lambs, with a particular emphasis on the IMF accumulation. Additionally, the transcriptomic and metabolomic tools were further used to increase our understanding of the cascade relationship from genes to phenotypes.

## 2. Materials and methods

### 2.1. Animal ethics statement

The study was conducted according to the Animal Welfare and Ethics Committee of Ningxia University (permission number: NXUC20200618). All breeding procedures and experimental protocols adhered to the guidelines outlined in Farm Animal Welfare Requirements: Mutton Sheep (T/CAS 242—2015), and received approval from the College of Animal Science and Technology, Ningxia University. We also confirmed that all experiments were compliant with the Animal Research Reporting of In Vivo Experiments (ARRIVE) guidelines.

### 2.2. FLBR preparation procedure

One ton of LBR (Beryl Wolfberry Limited by Share Ltd., Yinchuan, China) was ground into uniform powder and then mixed with 100 kg of water and 20 kg of sugarcane molasses. A combined inoculant (North Minzu University, Yinchuan, China), including 3 g $\times$ 5.0 $\times$ $10^9$ CFU/g *B. subtilis*, 5 g $\times$ 2.0 $\times$ $10^8$ CFU/g *Candida utilis* and 5 g $\times$ 1.2 $\times$ $10^{10}$ CFU/g *Saccharomyces cerevisiae* was added to the mixture. The resulting blend was then fermented in a fermenter (RK, SUOTE Machinery, China) equipped with an air sterile filter unit for 10 days. After fermentation, the residues were transferred to fermentation bags with a single breather valve (Hualiang Packaging, Guangzhou, China) and sealed using a vacuum packaging machine. Finally, the respective LBR and FLBR were uniformly mixed with basic diet, which was then processed into pellets (5 mm in diameter, 12.5 mm in length) before feeding.

### 2.3. Experimental animals and design

Eighteen healthy male Tan lambs (Tianyuan Well-Bred Lambs Breeding Co., Ltd., Wuzhong, China) with an average body weight of 19.97 $\pm$ 0.51 kg and an average age of 3.5 months were selected in this study. All lambs were randomly divided into three groups with 6 replicates (pens) per group: the control group (CON), LBR group, and fermented *L. barbarum* residues (FLBR) group. The CON received a basal diet, while the two treatment groups were fed a basal diet containing 5.0% (w/w) of LBR or FLBR for a duration of 90 days. The basal diets were formulated to meet the nutritional requirements of meat-type sheep and goats, as outlined in the Agricultural Industry Standard of China (NY/T 816—2021; Table 1). These lambs were arranged based on the RAND function in Excel. Individual animals were treated as the experimental units. Each lamb was housed in an individual pen (6.5 m $\times$ 4.25 m $\times$ 2.65 m) with free access to water and food. In the following 102 days including a 12-d acclimation period, these lambs were fed twice daily at 08:00 and 17:00.

### 2.4. Growth parameters measurement and sample collection

The body weight (BW) was measured on days 0, 45 and 90 before morning feeding, and the average daily gain (ADG) was calculated. Daily feed amount and feed leftover were recorded to compute the average daily feed intake (ADFI). Feed efficiency was determined as the ratio of ADG to ADFI. On the last day before slaughter, the body length, body height, chest circumference and shoulder width were measured following a standardized method (Lopez-Carlos et al., 2010). The blood samples were collected at 07:00 on the last day of the trial, and centrifugated at 3500 $\times$ *g*, 4 °C for 15 min to obtain serum, which was stored at −20 °C for subsequent analysis. These lambs were transported to the experimental abattoir, and then immediately slaughtered by professionals using the Halal method after 12 h of lairage time (Zhang et al., 2022). Each lamb was housed in an individual pen during lairage. After slaughter, the organs were immediately weighed. Carcasses were then chilled (0 to 4 °C) for 36 h, after which the longissimus thoracis (LT) was harvested for evaluating meat quality. Within 15 min of slaughter, IMF was obtained following the 2 g of IMF per 100 g of LT tissue. After fat tissue removal, the 20-g LT and 10-g IMF

**Table 1**
Ingredients and nutrient levels of diets (%, dry matter basis).

| Item | CON diet | LBR diet | FLBR diet |
|---|---|---|---|
| **Ingredients** | | | |
| Ground corn grain | 37.10 | 37.30 | 37.50 |
| Wheat straw | 15.30 | 13.30 | 14.00 |
| Alfalfa hay | 21.50 | 19.50 | 18.90 |
| Soybean meal | 13.40 | 12.30 | 11.90 |
| Soybean oil | 3.18 | 3.15 | 3.13 |
| Salt | 0.92 | 1.00 | 1.02 |
| Dicalcium phosphate | 0.45 | 0.45 | 0.42 |
| Calcium carbonate | 0.40 | 0.40 | 0.43 |
| Sodium bicarbonate | 1.00 | 1.00 | 1.00 |
| Premix[1] | 4.25 | 4.25 | 4.25 |
| Linseed | 2.55 | 2.35 | 2.45 |
| LBR | 0.00 | 5.00 | 0.00 |
| FLBR | 0.00 | 0.00 | 5.00 |
| Total | 100.05 | 100.00 | 100.00 |
| **Nutrient levels** | | | |
| OM | 88.80 | 89.70 | 89.50 |
| CP | 12.78 | 12.74 | 12.81 |
| EE | 6.10 | 5.75 | 5.84 |
| NDF | 36.20 | 35.80 | 35.63 |
| ADF | 19.45 | 19.25 | 19.38 |
| Calcium | 0.63 | 0.63 | 0.64 |
| Phosphorus | 0.40 | 0.40 | 0.40 |

LBR = *L. barbarum* residues; FLBR = fermented *L. barbarum* residues; CON = basal diet without supplementation with LBR or FLBR; DM = dry matter; OM = organic matter; CP = crude protein; EE = ether extract; NDF = neutral detergent fiber; ADF = acid detergent fiber.
[1] Premix in per kilogram of diet provided 100,000 IU, vitamin A, 20,000 IU, vitamin $D_3$, 60 IU, vitamin E, 1000 mg Fe, 1000 mg Mn, 780 mg Zn, 270 mg Cu, 12 mg Se and 10 mg I.

samples were separately mixed with RNAlater (R0118, Beyotime Biotechnology, Shanghai, China) and stored at 4 °C for 36 h, followed by transfer to a freezer at −80 °C until transcriptomic analysis. Concurrently, 20 g of LT samples were directly transferred to a freezer at −80 °C until UHPLC-MS/MS analysis. The rumen chyme was sequentially filtered through four layers of cheesecloth and filter paper to obtain rumen fluid, which was then analyzed for chemical parameters.

### 2.5. Determination of nutritional composition of feed containing LBR and FLBR

The nutritional composition and in vitro antioxidant properties of LBR and FLBR are presented in Table S1. The quantification of dry matter (DM), crude protein (CP) and ether extract (EE) in the feed were conducted according to AOAC (2000) using methods 934.01 for DM, 954.01 for CP and 920.39 for EE. The respective calcium and phosphorus of feed were measured in compliance with China National Standards (GB/T 6436-2018 and GB/T 6437-2018). Neutral detergent fiber (NDF) and acid detergent fiber (ADF) contents were measured using the F57 fiber bag (25 mm porosity) technique (ANKOM Technology, Fairport, NY, USA), adhering to the China National Standard (GB/T 20806-2022) and the Agricultural Industry Standard of China (NY/T 1459−2022), respectively. During NDF analysis, heat stable alpha-amylase and sodium sulfite were separately introduced to eliminate the effects of starch and protein.

### 2.6. Serum biochemical indicators, muscle antioxidant traits and rumen fermentation parameters

Serum biochemical indicators, including total protein (TP), albumin (ALB), globulin (GLB), urea nitrogen (UN), glucose (GLU), triacylglycerol (TG) and total cholesterol (TC) were measured using an AU400 Clinical Biochemistry Analyzer (Olympus Inc., Tokyo, Japan). Muscle antioxidant status was evaluated through the determination of total antioxidant capacity (T-AOC), malondialdehyde (MDA), superoxide dismutase (SOD) and catalase (CAT) according to the manufacturer's protocols (Nanjing Jiancheng Bioengineering Institute, Nanjing, China). The pH of the rumen fluid was measured using a hand-held pH meter (Testo 205, Germany). The ammonia-nitrogen ($NH_3$—N) concentration was quantified by the phenol sodium hypochlorite colorimetric method (Licitra et al., 1996). Acetate, propionate, butyrate, isobutyrate and isovalerate concentrations were measured using Gas chromatography (GC-2000A, Shimadzu Technologies Inc., Tokyo, Japan) based on an established protocol (Adorno et al., 2014).

### 2.7. Digestibility measurement

The feces were collected from days 86 to 90 of the trial to determine the nutrient digestibility. During the final 4 days of the trial, all lambs were housed in custom-designed metabolic cages. Every day, the total faeces excreted by each lamb over a 24-h period were gathered prior to the morning feeding, and the weight was carefully recorded. The fecal samples were then mixed with 5% (v/v) sulfuric acid at a ratio of 10:1 (w/v) and preserved in a refrigerator at −20 °C. A composite sample of 350 g was prepared by pooling 40 g of feces per 100 g of total excreted feces. These samples were subsequently dried at 65 °C for 72 h using an air-circulating oven with constant temperature control (101-0DB, TEISITE Instrument, Tianjin, China). Three technical replicates were set for each biological replicate. Analyses of DM, organic matter (OM), CP and EE in the feces were performed according to AOAC standard methods (AOAC, 2000; Method 934.01 for DM; Method 954.01 for CP, Method 920.39 for EE, Method 942.05 for ash). Organic matter was calculated as the difference between DM and ash. During the digestibility period, the feed amount and feed remaining were recorded for calculating feed ingested (Nm). The feces excreted amount (Ne), nutrient concentration in feed (Nd, %DM), and nutrient concentration in feces excreted (Nf, %DM) were recorded. The nutrient digestibility was calculated through the following formula:

$$\text{Nutrient digestibility } (\%) = \frac{\text{Nm} \times \text{Nd} - \text{Ne} \times \text{Nf}}{\text{Nm} \times \text{Nd}} \times 100$$

### 2.8. Meat quality and nutrients measurement

After the carcasses were suspended at 4 °C for 36 h, LT tissue between the 8th and 13th ribs was excised, trimmed of fat, and vacuum sealed at 4 °C for evaluating the meat quality. According to a modified method (Biffin et al., 2020), a 5-g sample (12th to 13th rib) was blended with 45 mL ultrapure water, which was then homogenized and suspended in a water bath until the temperature reached 23 °C. The pH electrode (Testo 205, Germany) was calibrated at 23 °C using standard solutions of pH 6.86 and 4.01, the post-mortem pH values were measured at 45 min and 24 h. The post-mortem parameters, including color, drip loss, water holding capacity (WHC), cooked meat rate (CMR) and shear force were measured as previously described (Zhang et al., 2022). In order to eliminate the air oxidation-caused color changes, the additional samples (12th to 13th rib) were blooming for 45 min prior to color analysis. Then, the colors at 0, 1 and 4 d were measured using CR-400 colorimeter (KONICA MINOLTA Co., Ltd., Tokyo, Japan) in accordance with lightness (L*), redness (a*) and yellowness (b*) by setting D65 illuminant, 8 mm measuring aperture size, and 2° observer angle. Each sample was tested three times at different positions.

For drip loss, muscle samples (2 cm × 2 cm × 4 cm) from the 9th to 10th rib were weighed, placed in inflatable plastic packages and then suspended at 4 °C for 24 h. The samples were then re-weighed to calculate the drip loss. Muscle samples at the 8th/9th rib were weighed and subjected to compression under a 35-kg of pressure for 5 min using RH-1000 Pressurizer (Runhu Instrument Co., Ltd., Guangzhou, China), after which they were re-weighed to calculate the WHC. After removing connective and fat tissues, the pre-cook weight of muscle samples (10 cm × 6 cm × 1 cm) between the 10th and 12th ribs was recorded. Then, these samples were sealed in plastic packages and a thermometer was inserted into the geometric center. Then, the samples were heated in an −80 °C thermostat water bath for 35 min until the internal temperature reached 70 °C. After cooled to indoor temperature, the post−cook weight of the samples was recorded for calculating the CMR. Subsequently, these cooked samples were trimmed into rectangles (3 cm × 1 cm × 1 cm) along a direction parallel to the muscle fibers, and shear force values were obtained by shearing towards a direction perpendicular to muscle fibers using a C-LM tenderness meter (MATTHAUS Co., Ltd., Germany). This trial used one cooking batch (3 technical replicates per sample) to eliminate the effects of the batch.

Analyses of nitrogen and ash of meat were performed according to AOAC (2006) using Method 928.08 for nitrogen, and Method 920.153 for ash. The muscular protein (MP) content was calculated as nitrogen × 6.25. Intramuscular fat content in meat was determined using the Soxhlet extraction method modified by Zhan et al. (2022). The concentration of muscular glycogen (MG) was determined following the instructions of the reagent kit (Nanjing Jiancheng Bioengineering Institute, Nanjing, China).

### 2.9. Total RNA extraction, library construction, and transcriptomic analysis for LT and IMF

RNA-Seq was performed on the Illumina NovaSeq 6000 platform by Novogene Co., Ltd. (Beijing, China). Total RNA was extracted from LT and IMF tissues using the RNA reagent kit (AM1561, Ambion, USA). RNA integrity and its quantity were evaluated using the Agilent 2100 Bioanalyzer (Agilent Technologies, CA, USA). The eukaryotic mRNA was enriched through Oligo (dT) beads based on the typical PolyA tail structure. The cDNA synthesis was performed in two consecutive reactions: the M-MuLV reverse transcriptase system and the DNA polymerase I system with mRNA segments serving as the template. After the ends repair and tail addition, the cDNA fragments of 250 to 300 bp were amplified by PCR, and then PCR products were purified using AMPure XP beads to construct the final library. After the library concentration was diluted to 1.5 ng/μL, insert size was assessed using the Agilent 2100 Bioanalyzer, and the library concentration was quantified by quantitative real-time polymerase chain reaction (qRT-PCR) to ensure it exceeded 2 nmol/L.

After filtering the reads with adapter or ploy-N and low-quality reads, the high-quality clean sequences were accurately mapped to the *Ovis aries* (sheep) reference genome using HISAT2 (https://daehwankimlab.github.io/hisat2/). Gene relative expression abundances were estimated as a fragment per kilobase of transcript per million mapped reads (FPKM). Differential gene expression analysis was performed using DESeq2, which calculated the fold change (FC) and *P*-values. False discovery rate (FDR) < 0.05, DESeq2 *P*-value < 0.05 and $|\log_2 FC| > 1$ were considered as the filters of differentially expressed genes (DEGs). According to *P*-value <0.05 of Fisher's exact test and $\chi 2$ test with ClusterProfile, all DEGs were annotated to the Gene Ontology (GO) database (http://geneontology.org/) for functional classification. Under the same threshold, enrichment analysis of DEGs was conducted using the online Kyoto Encyclopedia of Genes and Genomes (KEGG) database (http://www.genome.jp/kegg/) to identify relevant metabolic pathways. The protein−protein interaction (PPI) network of DEGs was further established by the STRING database (https://ngdc.cncb.ac.cn/). Pearson's correlation analysis was performed using GraphPad Prism 9.0 software.

### 2.10. Metabolites extraction, UHPLC-MS/MS, and metabolomic analysis

The 50-mg LT samples were mixed with 1000 μL of extracting solution (acetonitrile:methanol:water = 2:2:1, v:v:v) containing internal standard mixture of isotopes (13 C, 15 N and 2 H). Subsequently, the mixture was incubated at −40 °C for 1 h and then sonicated in an ice-water bath for 10 min. Next, the extracts were centrifuged at 13,000 × *g*, 4 °C for 20 min for obtaining supernatant to be tested. The metabolites in LT were separated using a UHPLC system (Vanquish, Thermo Fisher Scientific, USA) equipped with a UHPLC BEH Amide column (2.1 mm × 100 mm, 1.7 μm). The mobile phase was composed of 25 mmol/L ammonium acetate and 25 mmol/L ammonia hydroxide in water (pH = 9.75, solvent A) and acetonitrile (solvent B). The elution gradients were set as follows: 0 to 0.5 min, 95% B; 0.5 to 7.0 min, 95% to 65% B; 7.0 to 8.0 min, 65% to 40% B; 8.0 to 9.0 min, 40% B; 9.0 to 9.1 min, 40% to 95% B; 9.1 to 12.0 min, 95% B. The sampler temperature was 4 °C, and the injection volume was 2 μL. The column temperature was 25 °C. The flow rate was 0.5 mL/min. The effluent was introduced into a high-resolution mass spectrometry (Q Exactive HFX Orbitrap, Thermo Fisher Scientific, USA) by electrospray ionization. Electrospray ionization -Q-TOF-MS was applied on an information-dependent basis in both positive and negative ion modes with the following conditions: gas I, 60 psi; gas II, 60 psi; curtain gas, 35 psi; source temperature, 600 °C; decluttering potential, 60 V; ion-spray voltage, 5000 V (positive) and −4000 V (negative).

The positive and negative data were merged and normalized using quality control (QC) samples containing internal standards. The raw data were converted to the mzXML format using ProteoWizard, which were then used to process peak deconvolution, alignment and integration, retention time and correction using R package XCMS 3.2. SIMCA 15.0.2 (Sartorius Stedim, Sweden) was used to perform principal component analysis (PCA) and orthogonal projections to latent structures-discriminant analysis (OPLS-DA). The validity and reliability of OPLS-DA model were verified by performing 7-fold permutation tests. A reliable PCA model was shown as $R^2X > 0.5$. The $R^2Y$ and $Q^2$ values near 1.0 indicated an available OPLS-DA model. To identify significantly differential metabolites (DMs), the screening thresholds were set as follows: |FC| >1.0, variable importance in the projection (VIP) > 1.0 from the OPLS-DA model and the $P < 0.05$ of Student's *t*-test. The DMs were enriched to relevant pathways using MetaboAnalyst 4.0 (http://www.metaboanalyst.ca/). Hierarchical clustering analysis of the DMs was performed using Cluster 3.0 software.

### 2.11. Statistics analysis

All data were showed as means ± standard error of the mean (SEM). Normality of data distribution was tested using Shapiro Wilk test, and skewed data sets were log-transformed. The data on growth parameters, serum biochemical indicators, muscle antioxidant capacity, meat quality, muscular nutrient, rumen fermentation parameters and nutrient digestibility were analyzed using the MIXED procedure by IBM-SPSS 26.0 (SPSS Inc., Chicago, IL, USA). The dietary treatment was considered as a fixed variable and the individual animal was a random variable according to the linear mixed-effects model:

$$y_{ij} = \mu + D_i + P_j + e_{ij},$$

where $\mu$ is general mean; $D_i$ is the fixed effect of diet ($i$ = CON, LBR, FLBR); $P_j$ is the random effect of the individual animal; $e_{ij}$ is the residual error. Duncan's multiple comparison tests were performed to compare the differences between treatments. A statistical significance was showed as $P$-value <0.05, and a tendency was considered as 0.05 < $P$-value < 0.10.

## 3. Results

### 3.1. Effects of FLBR supplementation on the growth parameters, serum biochemical indicators, and muscle antioxidant trait of lambs

The lambs fed with the FLBR diet exhibited significantly higher ADG ($P$ = 0.008), feed efficiency ($P$ = 0.007), and 90-d BW ($P$ = 0.019) compared to the CON and LBR diets (Table 2). Additionally, the lambs in FLBR group had higher levels of serum TP, ALB, GLB, GLU and TG ($P$ < 0.05 or $P$ < 0.01), along with reduced serum UN levels ($P$ = 0.001; Table 3). FLBR supplementation significantly increased muscle T-AOC ($P$ < 0.001) and SOD activity ($P$ = 0.003), but reduced muscle MDA content ($P$ < 0.001; Table 3).

### 3.2. Effects of FLBR supplementation on the rumen fermentation characteristics, and nutrient digestibility of lambs

As illustrated in Table 4, FLBR supplementation significantly increased acetate ($P$ = 0.002) and propionate ($P$ = 0.011) concentrations versus the CON or LBR, but significantly decreased $NH_3$–N ($P$ = 0.002), isobutyrate ($P$ = 0.030) and isovalerate concentrations ($P$ < 0.001). The digestibility of OM, CP, EE, NDF and ADF was significantly higher due to FLBR supplementation ($P$ < 0.05; Table 5).

**Table 2**
The growth parameters and organs weight of lambs ($n$ = 6).

| Item | Treatments | | | SEM | $P$-value |
|---|---|---|---|---|---|
| | CON | LBR | FLBR | | |
| **Growth performance** | | | | | |
| 0–90 d ADFI, g/d | 1684.65 | 1681.98 | 1677.80 | 8.746 | 0.955 |
| Initial BW, kg | 20.02 | 19.93 | 19.97 | 0.120 | 0.965 |
| 0 d BW, kg | 20.83 | 20.85 | 20.84 | 0.107 | 0.999 |
| 45 d BW, kg | 28.22 | 28.03 | 28.57 | 0.153 | 0.367 |
| 90 d BW, kg | 36.16$^{b}$ | 35.84$^{b}$ | 37.02$^{a}$ | 0.189 | 0.019 |
| 0–90 d ADG, g/d | 170.33$^{b}$ | 166.56$^{b}$ | 179.74$^{a}$ | 1.934 | 0.008 |
| Feed efficiency | 0.101$^{b}$ | 0.099$^{b}$ | 0.107$^{a}$ | 0.031 | 0.007 |
| **Body size parameters, cm** | | | | | |
| Body length | 69.92$^{b}$ | 68.62$^{b}$ | 73.06$^{a}$ | 0.670 | 0.011 |
| Body height | 61.12 | 62.55 | 64.33 | 0.591 | 0.075 |
| Chest circumference | 77.70 | 79.22 | 81.15 | 0.630 | 0.072 |
| Left forearm circumference | 7.97 | 6.92 | 7.28 | 0.216 | 0.128 |
| Shoulder width | 22.22 | 20.10 | 20.80 | 0.401 | 0.082 |
| **The organs weight, g** | | | | | |
| Heart | 161.83 | 162.50 | 168.67 | 1.811 | 0.248 |
| Liver | 679.30 | 691.67 | 707.33 | 5.004 | 0.063 |
| Spleen | 73.10$^{b}$ | 70.18$^{b}$ | 84.67$^{a}$ | 2.551 | 0.037 |
| Lung | 482.17 | 472.50 | 467.67 | 3.922 | 0.326 |
| Kidney | 87.27 | 92.00 | 93.67 | 1.871 | 0.359 |
| Rumen | 612.80$^{b}$ | 604.83$^{b}$ | 625.17$^{a}$ | 3.431 | 0.040 |
| Reticulum | 102.83 | 97.67 | 99.33 | 1.674 | 0.464 |
| Omasum | 116.67 | 110.83 | 125.17 | 2.550 | 0.060 |
| Abomasum | 174.33 | 178.50 | 184.50 | 2.287 | 0.195 |

LBR = *L. barbarum* residues; FLBR = fermented *L. barbarum* residues; CON = basal diet without supplementation of LBR or FLBR; SEM = standard error of the mean; ADFI = average daily feed intake; BW = body weight; ADG = average daily gain. Different lowercase letters means significant difference, $P$ < 0.05.

**Table 3**
Serum biochemical parameters and muscle (longissimus thoracis) antioxidant indicators of lambs ($n$ = 6).

| Item | Treatments | | | SEM | $P$-value |
|---|---|---|---|---|---|
| | CON | LBR | FLBR | | |
| **Serum** | | | | | |
| TP, g/L | 56.53$^{b}$ | 55.94$^{b}$ | 61.34$^{a}$ | 0.844 | 0.007 |
| ALB, g/L | 26.23$^{b}$ | 25.56$^{b}$ | 28.52$^{a}$ | 0.458 | 0.011 |
| GLB, g/L | 28.47$^{b}$ | 29.86$^{ab}$ | 32.23$^{a}$ | 0.621 | 0.032 |
| UN, mmol/L | 7.23$^{a}$ | 8.15$^{a}$ | 6.07$^{b}$ | 0.272 | 0.001 |
| GLU, mmol/L | 5.80$^{b}$ | 5.55$^{b}$ | 6.83$^{a}$ | 0.182 | 0.002 |
| TC, mmol/L | 1.91 | 1.85 | 2.01 | 0.052 | 0.458 |
| TG, mmol/L | 0.30$^{ab}$ | 0.26$^{b}$ | 0.36$^{a}$ | 0.016 | 0.027 |
| **Muscle** | | | | | |
| T-AOC, μmol Trolox/g fresh weight | 0.69$^{b}$ | 0.75$^{b}$ | 1.02$^{a}$ | 0.045 | <0.001 |
| MDA, nmol/mg prot | 1.29$^{a}$ | 1.11$^{b}$ | 1.01$^{b}$ | 0.038 | <0.001 |
| SOD, U/mg prot | 98.78$^{b}$ | 113.17$^{b}$ | 131.32$^{a}$ | 4.162 | 0.003 |
| CAT, U/mg prot | 32.32 | 34.22 | 31.34 | 1.130 | 0.599 |

LBR = *L. barbarum* residues; FLBR = fermented *L. barbarum* residues; CON = basal diet without supplementation of LBR or FLBR; SEM = standard error of the mean; TP = total protein; ALB = albumin; GLB = globulin; UN = urea nitrogen; GLU = glucose; TC = total cholesterol; TG = triacylglycerol; T-AOC = total antioxidant capacity; MDA = malondialdehyde; SOD = superoxide dismutase; CAT = catalase. Different lowercase letters means significant difference, $P$ < 0.05.

**Table 4**
Rumen fermentation parameters of lambs ($n$ = 6).

| Item | Treatments | | | SEM | $P$-value |
|---|---|---|---|---|---|
| | CON | LBR | FLBR | | |
| pH | 6.82 | 6.81 | 6.73 | 0.030 | 0.443 |
| $NH_3$–N, mg/100 mL | 14.12$^{b}$ | 15.33$^{a}$ | 12.69$^{c}$ | 0.331 | 0.002 |
| Acetate, mmol/L | 15.04$^{b}$ | 15.71$^{b}$ | 17.89$^{a}$ | 0.377 | 0.002 |
| Propionate, mmol/L | 8.86$^{b}$ | 8.09$^{b}$ | 10.52$^{a}$ | 0.351 | 0.011 |
| Butyrate, mmol/L | 1.87 | 1.93 | 1.97 | 0.087 | 0.905 |
| Isobutyrate, mmol/L | 0.78$^{b}$ | 1.11$^{a}$ | 0.72$^{b}$ | 0.067 | 0.030 |
| Isovalerate, mmol/L | 1.07$^{b}$ | 1.30$^{a}$ | 0.79$^{c}$ | 0.062 | <0.001 |
| Acetate/propionate | 1.71 | 1.97 | 1.69 | 0.059 | 0.137 |

LBR = *L. barbarum* residues; FLBR = fermented *L. barbarum* residues; CON = basal diet without supplementation of LBR or FLBR; SEM = standard error of the mean. Different lowercase letters means significant difference, $P$ < 0.05.

### 3.3. Effects of FLBR supplementation on the meat quality and nutrient contents of lambs

Table 6 demonstrated that supplementation with FLBR significantly decreased post-mortem drip loss ($P$ = 0.001) and shear force ($P$ = 0.008) versus the CON or LBR diet. Lambs in the FLBR group had significantly higher post-mortem color $a^*$, pH and WHC than those in the CON or LBR groups ($P$ < 0.05 or $P$ < 0.001). Additionally, the inclusion of FLBR in the diet resulted in significantly higher MP ($P$ = 0.003), IMF ($P$ = 0.001), and MG ($P$ = 0.011) contents versus the CON or LBR groups.

**Table 5**
Nutrient digestibility of lambs ($n$ = 6) (%).

| Item | Treatments | | | SEM | $P$-value |
|---|---|---|---|---|---|
| | CON | LBR | FLBR | | |
| OM | 56.13$^{b}$ | 54.89$^{b}$ | 61.28$^{a}$ | 0.789 | <0.001 |
| CP | 65.06$^{b}$ | 63.02$^{b}$ | 69.25$^{a}$ | 0.694 | 0.002 |
| EE | 53.18$^{b}$ | 51.79$^{b}$ | 55.94$^{a}$ | 0.584 | 0.010 |
| NDF | 48.67$^{b}$ | 49.98$^{b}$ | 52.96$^{a}$ | 0.606 | 0.004 |
| ADF | 33.57$^{b}$ | 35.13$^{ab}$ | 36.44$^{a}$ | 0.432 | 0.014 |

LBR = *L. barbarum* residues; FLBR = fermented *L. barbarum* residues; CON = without supplementation of LBR or FLBR; SEM = standard error of the mean; OM = organic matter; CP = crude protein; EE = ether extract; NDF = neutral detergent fiber; ADF = acid detergent fiber.
Different lowercase letters means significant difference, $P$ < 0.05.

**Table 6**
Meat (longissimus thoracis) quality and muscular nutrient ingredient of lambs ($n = 6$).

| Item | Treatments | | | SEM | *P*-value |
|---|---|---|---|---|---|
| | CON | LBR | FLBR | | |
| Drip loss, % | 6.84[a] | 7.14[a] | 5.19[b] | 0.294 | 0.001 |
| WHC, % | 51.02[b] | 48.67[b] | 54.29[a] | 0.665 | <0.001 |
| CMR, % | 72.46 | 71.61 | 72.87 | 0.290 | 0.203 |
| Shear force, N | 51.84[a] | 53.66[a] | 47.52[b] | 0.904 | 0.008 |
| **pH value** | | | | | |
| 45 min | 6.33[b] | 6.27[b] | 6.57[a] | 0.036 | <0.001 |
| 24 h | 5.62[b] | 5.59[b] | 5.76[a] | 0.028 | 0.018 |
| **Meat color** | | | | | |
| $L^*_{0\ d}$ | 37.32 | 37.50 | 36.51 | 0.288 | 0.345 |
| $a^*_{0\ d}$ | 17.76[b] | 18.18[b] | 19.42[a] | 0.289 | 0.039 |
| $b^*_{0\ d}$ | 4.38 | 4.09 | 4.29 | 0.130 | 0.661 |
| $L^*_{1\ d}$ | 43.01 | 41.83 | 42.17 | 0.381 | 0.452 |
| $a^*_{1\ d}$ | 19.14[b] | 20.23[ab] | 20.79[a] | 0.271 | 0.028 |
| $b^*_{1\ d}$ | 6.93 | 7.28 | 6.39 | 0.210 | 0.235 |
| $L^*_{4\ d}$ | 44.28 | 43.69 | 42.83 | 0.300 | 0.129 |
| $a^*_{4\ d}$ | 16.27[b] | 16.83[b] | 17.92[a] | 0.197 | 0.011 |
| $b^*_{4\ d}$ | 9.13[a] | 8.84[a] | 7.78[b] | 0.172 | 0.008 |
| **Muscular nutrient**, % fresh weight | | | | | |
| MP, | 19.36[b] | 18.72[b] | 20.97[a] | 0.316 | 0.003 |
| IMF | 5.16[b] | 4.68[b] | 6.61[a] | 0.255 | 0.001 |
| MG | 0.96[b] | 0.90[b] | 1.05[a] | 0.023 | 0.011 |
| Ash | 3.67 | 3.50 | 3.78 | 0.052 | 0.071 |

LBR = *L. barbarum* residues; FLBR = fermented *L. barbarum* residues; CON = basal diet without supplementation of LBR or FLBR; SEM = standard error of the mean; WHC = water holding capacity; CMRFLA cooked meat rate; L* = lightness; a* = redness; b* = yellowness; MP = muscular protein; IMF = intramuscular fat; MG = muscular glycogen; DM = dry matter.
Different lowercase letters means significant difference, $P < 0.05$.

### 3.4. Transcriptomic profiles for LT and IMF tissues

The PCA analysis of all genes demonstrated that 6 replicates within per group exhibited little variations, but a good extent of separation was observed between groups for LT tissue (Fig. 1A). Under the principles of FDR ≤0.05, *P*-value <0.05 and $|\log_2 FC| \geq 1.0$, 654 DEGs (LBR vs CON) with 264 upregulated genes and 390 downregulated genes were identified (Fig. 1B); 962 DEGs (FLBR vs CON) were identified, where 416 DEGs were upregulated, and 546 DEGs were downregulated (Fig. 1C); 782 DEGs (FLBR vs LBR) were identified, where 405 DEGs were upregulated, and 377 DEGs were downregulated (Fig. 1D).

Fig. 1E demonstrated that there was little variation among the 6 replicates within each group, but clear separation between groups for IMF tissue. Under the same principles, 690 DEGs (LBR vs CON) with 417 upregulated genes and 273 downregulated genes were identified (Fig. 1F); 1313 DEGs (FLBR vs CON) were identified, where 604 DEGs were upregulated, and 709 DEGs were downregulated (Fig. 1G); 1221 DEGs (FLBR vs LBR) were identified, where 532 DEGs were upregulated, and 689 DEGs were downregulated (Fig. 1H).

### 3.5. FLBR and LBR affected GO function annotation and KEGG pathway enrichment of DEGs in LT

As illustrated in Fig. 2A, the DEGs between the LBR and CON were annotated to 11 biological processes, 4 cellular component, and 14 molecular functions. These DEGs were functionally related to amide metabolic process (GO:0043603), immune response and process (GO:0006955), ribonucleoprotein complex (GO:1990904) and

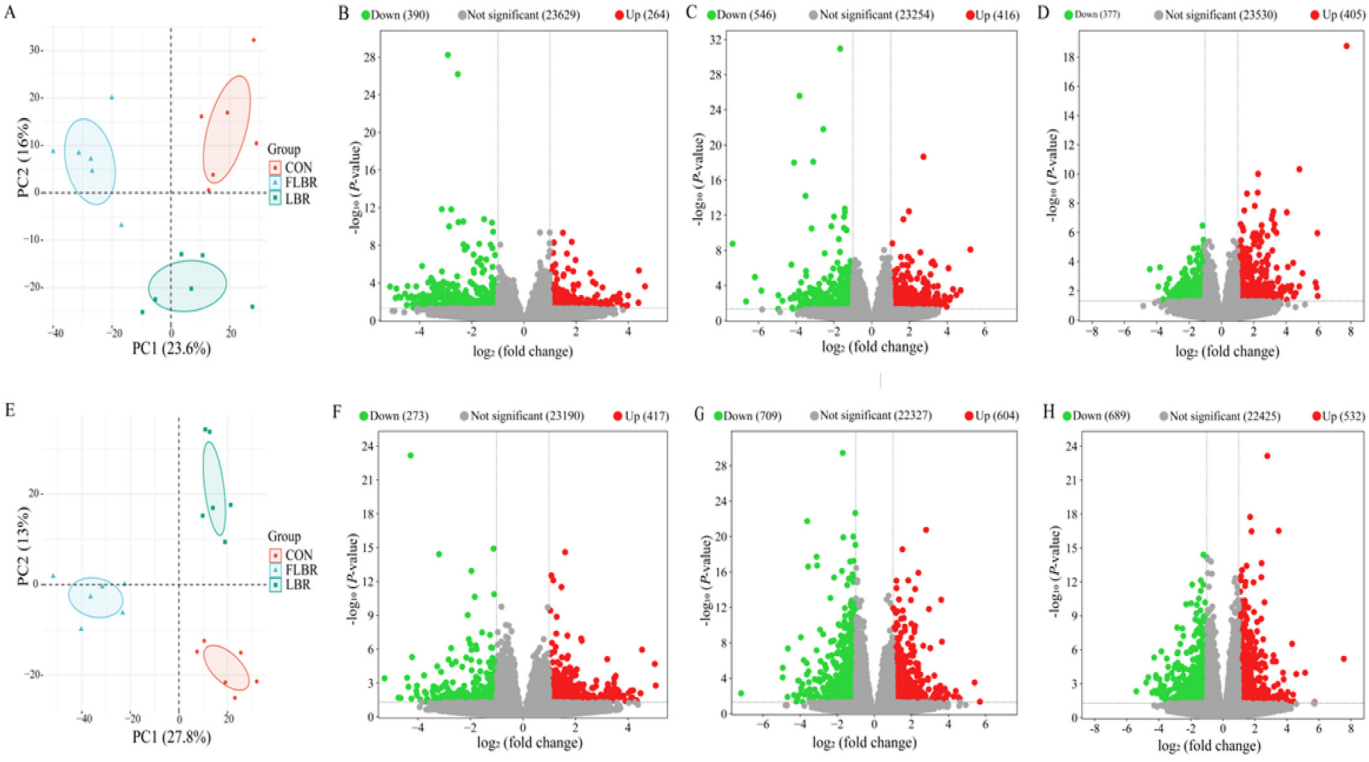


**Fig. 1. Effects of LBR and FLBR supplementation on transcriptomic profiles of LT and IMF tissues.** (A) PCA plot of DEGs in LT tissue. (B, C, D) Volcano plots of DEGs of LBR vs. CON, FLBR vs. CON and FLBR vs. LBR in LT tissue. (E) PCA plot of DEGs in IMF tissue. (F, G, H) Volcano plots of DEGs of LBR vs. CON, FLBR vs. CON and FLBR vs. LBR in IMF tissue. LBR = *L. barbarum* residues; FLBR = fermented *L. barbarum* residues; CON = basal diet without supplementation of LBR or FLBR; DEGs = differentially expressed genes; PCA = principal component analysis; LT = longissimus thoracis; IMF = intramuscular fat.

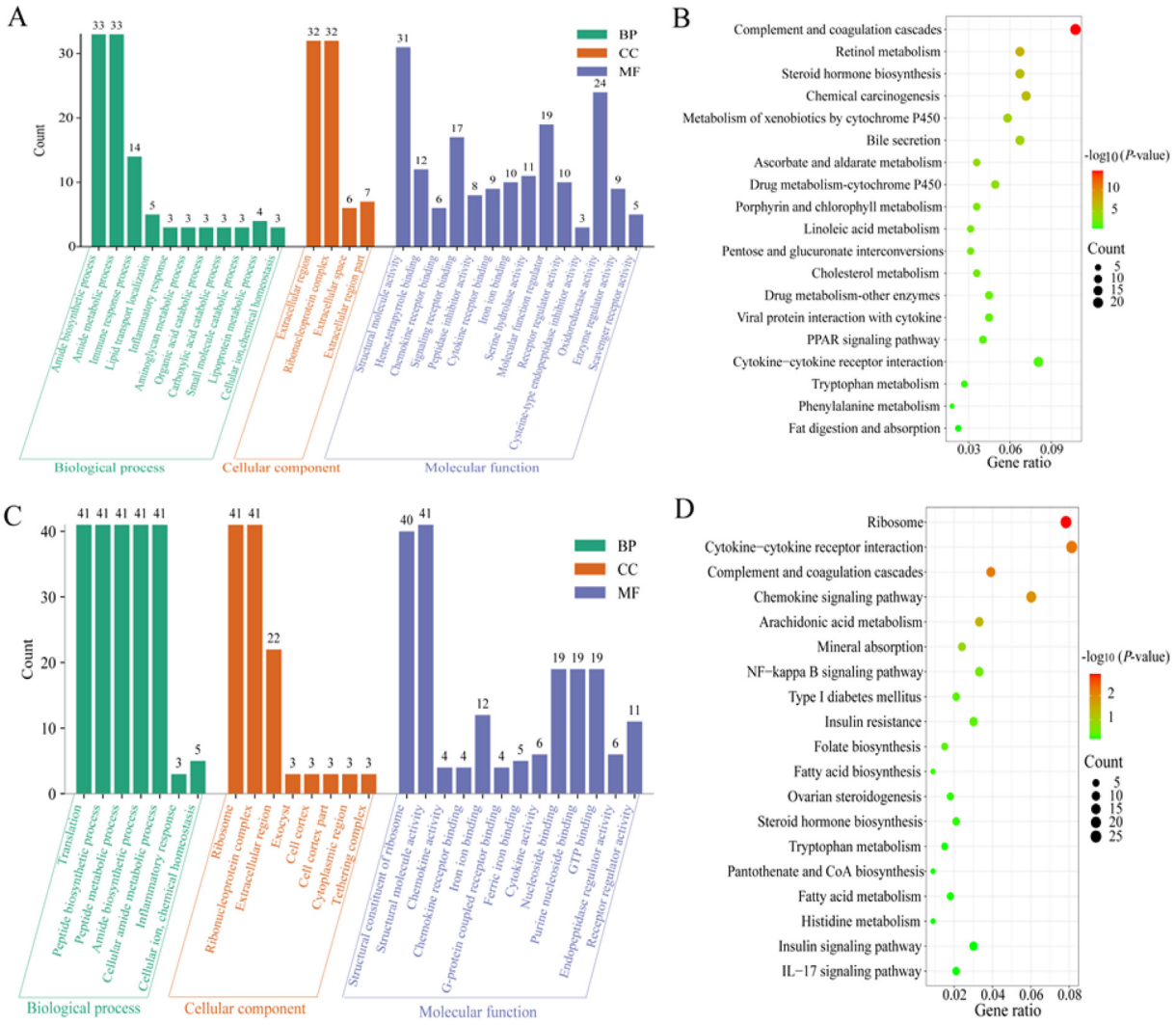


**Fig. 2. GO functional annotation and KEGG enrichment pathway of DEGs in LT.** (A, B) GO functional annotation and KEGG enrichment pathway of DEGs of LBR vs. CON; (C, D) GO functional annotation and KEGG enrichment pathway of DEGs of FLBR vs. CON. LBR = *L. barbarum* residues; FLBR = fermented *L. barbarum* residues; CON = basal diet without supplementation of LBR or FLBR; DEGs = differentially expressed genes; GO = Gene Ontology; KEGG = Kyoto Encyclopedia of Genes and Genomes; BP = biological process; CC = cellular component; MF = molecular function; LT = longissimus thoracis.

structural molecule activity (GO:0005198). The DEGs between the FLBR and CON groups were annotated to 28 GO subcategories including 7 biological processes, 8 cellular component, and 13 molecular functions (Fig. 2C). For biological process, these DEGs were annotated to translation (GO:0006412), peptide biosynthetic process (GO:0043043) and amide biosynthetic process (GO:0043604). The cellular component mainly included ribosome (GO:0005840), ribonucleoprotein complex (GO:1990904) and extracellular region (GO:0005576). The molecular function was primarily related to structural constituent of ribosome (GO:0003735) and structural molecule activity (GO:0005198). This annotation provides detailed insights into the functional implications of the DEGs, emphasizing the biological relevance of the observed gene expression changes in response to dietary variations.

KEGG pathway analysis revealed that the DEGs (LBR vs CON) were significantly enriched in 18 signaling pathways including Complement and coagulation cascades, Retinol metabolism, Chemical carcinogenesis and Chlorophyll metabolism, etc (Fig. 2B). Total of 26 DEGs (FLBR vs CON) in Ribosome pathway were all the corresponding genes of ribosomal protein biosynthesis (Fig. 2D), where 10 DEGs were up, and 16 DEGs were down. Furthermore, the DEGs between FLBR and LBR were significantly enriched in pathways such as Complement and coagulation cascades, Tyrosine metabolism, Retinol metabolism, Fatty acid biosynthesis, Phenylalanine metabolism (Fig. S1A).

### 3.6. FLBR and LBR affected GO function annotation and KEGG pathway enrichment of DEGs in IMF

Fig. 3A demonstrated that the DEGs between the LBR and CON were annotated to 24 GO subcategories, including 6 biological processes, 3 cellular components and 15 molecular functions, although no functional enrichment related to lipid metabolism was observed. The DEGs between the FLBR and CON groups were enriched to 25 GO subcategories including 7 biological processes, 6 cellular component and 12 molecular functions (Fig. 3C). Among these, inflammatory response (GO:0006954), cellular lipid metabolic process (GO:0044255) and fatty acid metabolic process (GO:0006631) were prominently represented.

KEGG enrichment analysis revealed that the DEGs between the LBR and CON were significantly enriched in several disease-related pathways such as Complement and coagulation cascades, Malaria

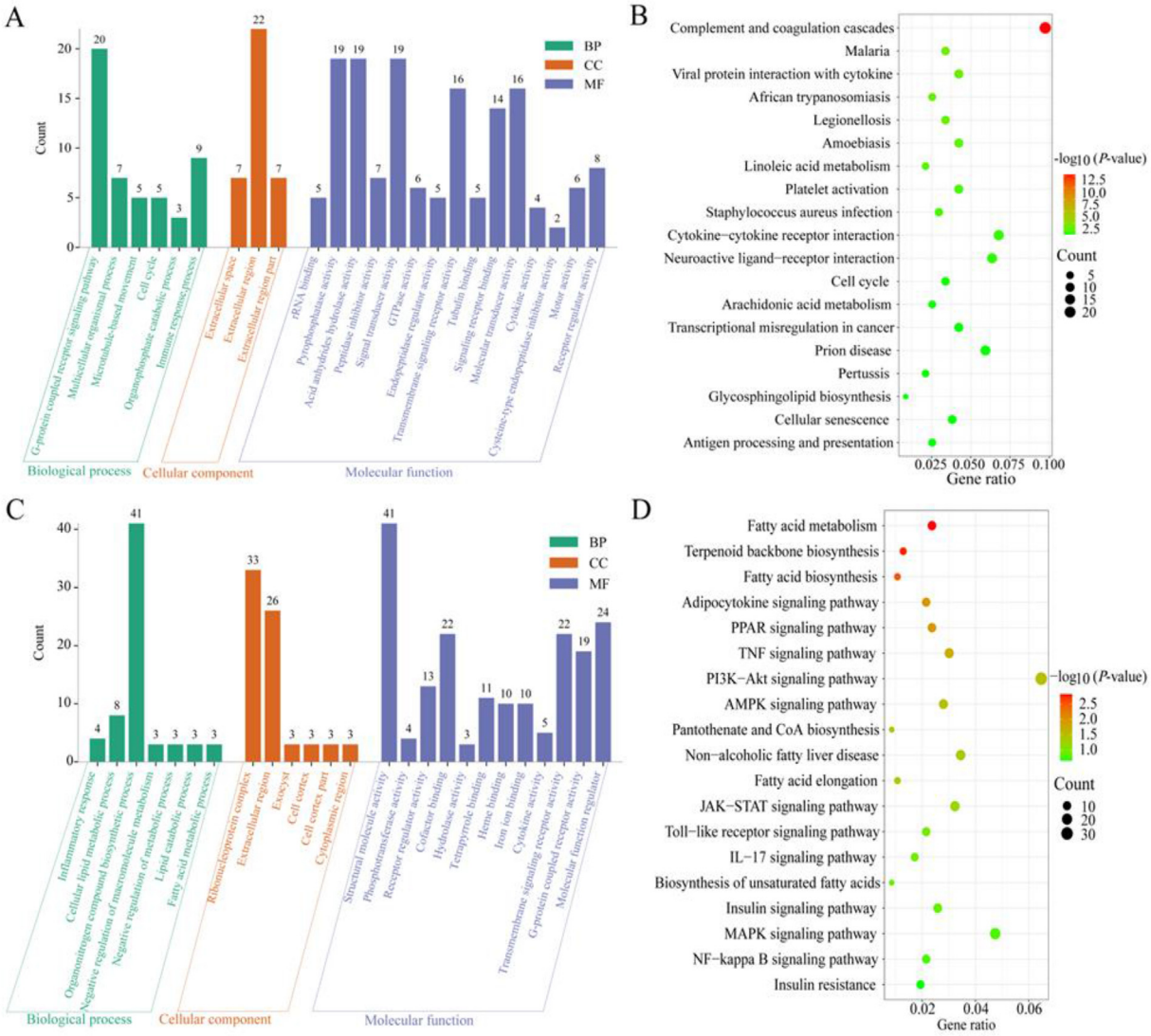


**Fig. 3. GO functional annotation and KEGG enrichment pathway of DEGs in IMF.** (A, B) GO functional annotation and KEGG enrichment pathway of DEGs of LBR vs. CON; (C, D) GO functional annotation and KEGG enrichment pathway of DEGs of FLBR vs. CON. LBR = *L. barbarum* residues; FLBR = fermented *L. barbarum* residues; CON = basal diet without supplementation of LBR or FLBR; DEGs = differentially expressed genes; GO = Gene Ontology; KEGG = Kyoto Encyclopedia of Genes and Genomes; BP = biological process; CC = cellular component; MF = molecular function. IMF = intramuscular fat.

and Legionellosis (Fig. 3B). Compared with the CON diet, FLBR intervention significantly triggered 6 potential pathways regulating lipid metabolism including Fatty acid metabolism, Fatty acid biosynthesis, Adipocytokine signaling pathway, PPAR signaling pathway, PI3K-Akt signaling pathway and Fatty acid elongation ($P < 0.05$; Fig. 3D). A total of 51 DEGs exhibited an obvious enrichment in the 6 metabolic processes, where 24 DEGs, such as *ACACA*, *LEP*, *ACSL6*, *ACAT2*, *FASN* and *ELOVL6*, were up, and 27 DEGs, such as *LEPR*, *ACSBG1*, *SOCS3*, *TNF*, *IL6* and *IL2RB*, were down. These DEGs between FLBR and LBR were significantly enriched in the PPAR signaling pathway, Fatty acid metabolism, Steroid biosynthesis and Adipocytokine signaling pathway (Fig. S1C).

### 3.7. Establishment of PPI network and correlation analysis

PPI network was employed to study the interaction and functional relationships among the DEGs. The 67 DEGs (FLBR vs CON) from LT tissue were used to perform PPI analysis (Table S2). An extremely close interaction network was established only among 17 DEGs including 11 genes involved in ribosomal protein biosynthesis and 6 pseudogenes lacking protein-coding function (Fig. 4A). Only 9 ribosomal protein genes (*RPL10A*, *RPL3*6AL, *RPL9*, *RPL26L*, *RPL35A*, *RPL13*, *RPL6*, *RPL36*, and *RPL17*) showed a significant correlation with the MP content ($P < 0.05$; Fig. 4B and Table 7). PPI analysis of DEGs (FLBR vs LBR) revealed that 30 DEGs were functionally related to the immune response, amino acid metabolism, fatty acid metabolism and xenobiotic metabolism, forming a close interaction network (Fig. S1B).

As shown in Table S3 and Fig. 4C, the 51 DEGs (FLBR vs CON) from 6 lipid metabolism-related signaling pathways established a close PPI network. Among these, 10 key DEGs, including *ACACA*, *LEP*, *LPL*, *CPT2*, *ACSL1*, *ACSL6*, *ACAT2*, *FASN*, *HSD17B12*, and *ELOVL6*, were significantly correlated with the IMF content ($P < 0.05$; Fig. 4D and Table 7). The 28 DEGs (FLBR vs LBR) were functionally associated with the lipid metabolism and highly interactive (Fig. S1D).

### 3.8. Metabolomic profiles for LT and KEGG pathway analysis

After data from the two modes were combined, the models remained to have accurate predictability and outstanding

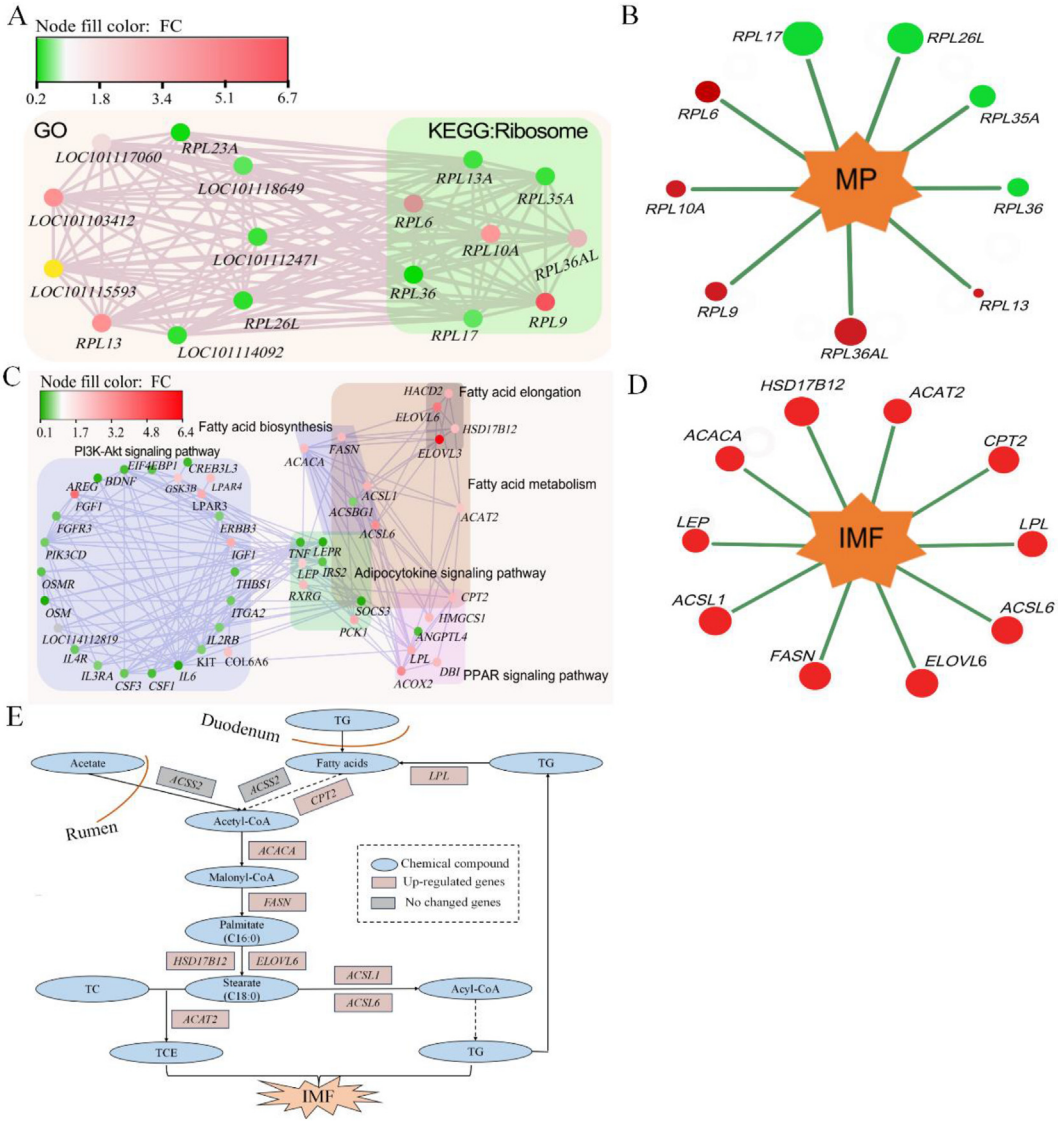


**Fig. 4. Protein–protein interaction (PPI) analysis of DEGs and Pearson's correlation analysis.** (A, C) The respective PPI analysis of DEGs in LT and IMF tissues; FC increased with node color changes from yellow to red. (B, D) Correlation analysis of DEGs with MP and IMF contents, respectively ($P < 0.05$); the larger red and green shapes represent extent of positive and negative correlation, respectively. (E) Schematic diagram on FLBR improved the IMF accumulation of lambs. FLBR = fermented *L. barbarum* residues; FC = fold change; DEGs = differentially expressed genes; MP = muscle protein; IMF = intramuscular fat; ACSS2 = acetyl-CoA synthetase 2; TCE = total cholesterol esters; TG = triglycerides.

availability ($R^2X = 0.525$ for PCA; $R^2Y = 1.000$ and $Q^2 = 0.975$ for OPLS-DA; Table S4). The PCA, OPLS-DA and clustering analysis of DMs (FLBR vs CON) exhibited that samples within the same group had similar metabolomic profiles, while distinct differences were observed between groups (Fig. 5A, B and E).

A total of 1732 DMs were identified by FC > 1.0, VIP >1.0 and *P*-value <0.05 after FLBR intervention, where 655 were upregulated, and 1077 were downregulated (Fig. 5C). KEGG enrichment analysis showed that these DMs were significantly enriched in pathways related to the Histidine metabolism, Arginine and proline metabolism, Aminoacyl-tRNA biosynthesis and Glycolysis (Fig. 6A). As illustrated in Tables S5 and S6, the increased metabolites mainly included L-histidine, carnosine, L-arginine, and L-proline in the FLBR compared with the CON, while the decreased metabolites were mainly citrulline, L-aspartic acid, phosphoenolpyruvic acid (PEP), and 2-Phospho-D-glyceric acid (2-p-D-ga). Most of these DMs showed significant correlations with meat quality indicators and MP content ($P < 0.05$ or $P < 0.01$; Fig. 6B). Based on Figs. S2, S3, S4 and S5, Fig. 6C showed that the interactions among metabolic pathways on FLBR improved the meat quality of lambs.

## 4. Discussion

### *4.1. FLBR improved growth performance by altering the rumen fermentation characteristics and nutrient digestibility of lambs*

The objective of this study was to explore physiological and molecular mechanisms behind the long-term effects of FLBR supplementation on the growth performance and meat quality of fattening lambs. A key aspect of the research was the comparative phenotypic effects and multi-omics analysis between the FLBR and LBR diets. No significant differences in phenotypic data were observed between the LBR and CON groups. However, lambs that received the FLBR diet exhibited significantly improved growth rates and feed efficiency. Rumen fermentation parameters reflect dietary nutrient digestion. Previous study has demonstrated that

**Table 7**
The key functional DEGs in LT and IMF tissues of lambs that received FLBR diet compared with CON diet.

| Type | Gene_ID | Gene symbols | Gene names | FC | FDR |
|---|---|---|---|---|---|
| LT | 101106166 | *RPL10A* | 60S ribosomal protein L10a | 2.04 | 0.0178 |
| | 101117063 | *RPL36AL* | 60S ribosomal protein L36a-like | 2.56 | 0.0126 |
| | 101107098 | *RPL9* | 60S ribosomal protein L9 | 6.69 | <0.0010 |
| | 101104237 | *RPL26L* | 60S ribosomal protein L26-like | −3.18 | <0.0010 |
| | 100037664 | *RPL35A* | 60S ribosomal protein L35a | −2.76 | <0.0010 |
| | 101113344 | *RPL13* | 60S ribosomal protein L13 %2C transcript variant *X*1 | 3.24 | 0.0192 |
| | 101109212 | *RPL6* | 60S ribosomal protein L6 | 2.04 | <0.0010 |
| | 101103232 | *RPL36* | 60S ribosomal protein L36 | −5.02 | 0.0045 |
| | 101115926 | *RPL17* | 60S ribosomal protein L17 %2C transcript variant *X*1 | −2.76 | <0.0010 |
| IMF | 443186 | *ACACA* | Acetyl-CoA carboxylase alpha | 2.38 | 0.0021 |
| | 443534 | *LEP* | Leptin | 2.01 | <0.0010 |
| | 443408 | *LPL* | Lipoprotein lipase%2C transcript variant *X*1 | 2.70 | <0.0010 |
| | 101118317 | *CPT2* | Carnitine palmitoyltransferase 2 | 2.46 | <0.0010 |
| | 101110905 | *ACSL1* | Acyl-CoA synthetase long chain family member 1 %2C transcript variant *X*2 | 2.59 | <0.0010 |
| | 101102389 | *ACSL6* | Acyl-CoA synthetase long chain family member 6 %2C transcript variant *X*1 | 3.36 | <0.0010 |
| | 101111975 | *ACAT2* | Acetyl-CoA acetyltransferase 2 | 2.19 | <0.0010 |
| | 100170327 | *FASN* | Fatty acid synthase | 2.44 | <0.0010 |
| | 101118274 | *ELOVL6* | ELOVL fatty acid elongase 6 %2C transcript variant *X*1 | 3.82 | <0.0010 |
| | 101110086 | *HSD17B12* | Hydroxysteroid L7-beta dehydrogenase L2 | 2.30 | <0.0010 |

FLBR = fermented *L. barbarum* residues; CON = basal diet without supplementation of LBR or FLBR; DEGs = differentially expressed genes; FC = fold change; FDR = false discovery rate; LT = longissimus thoracis; IMF = intramuscular fat.

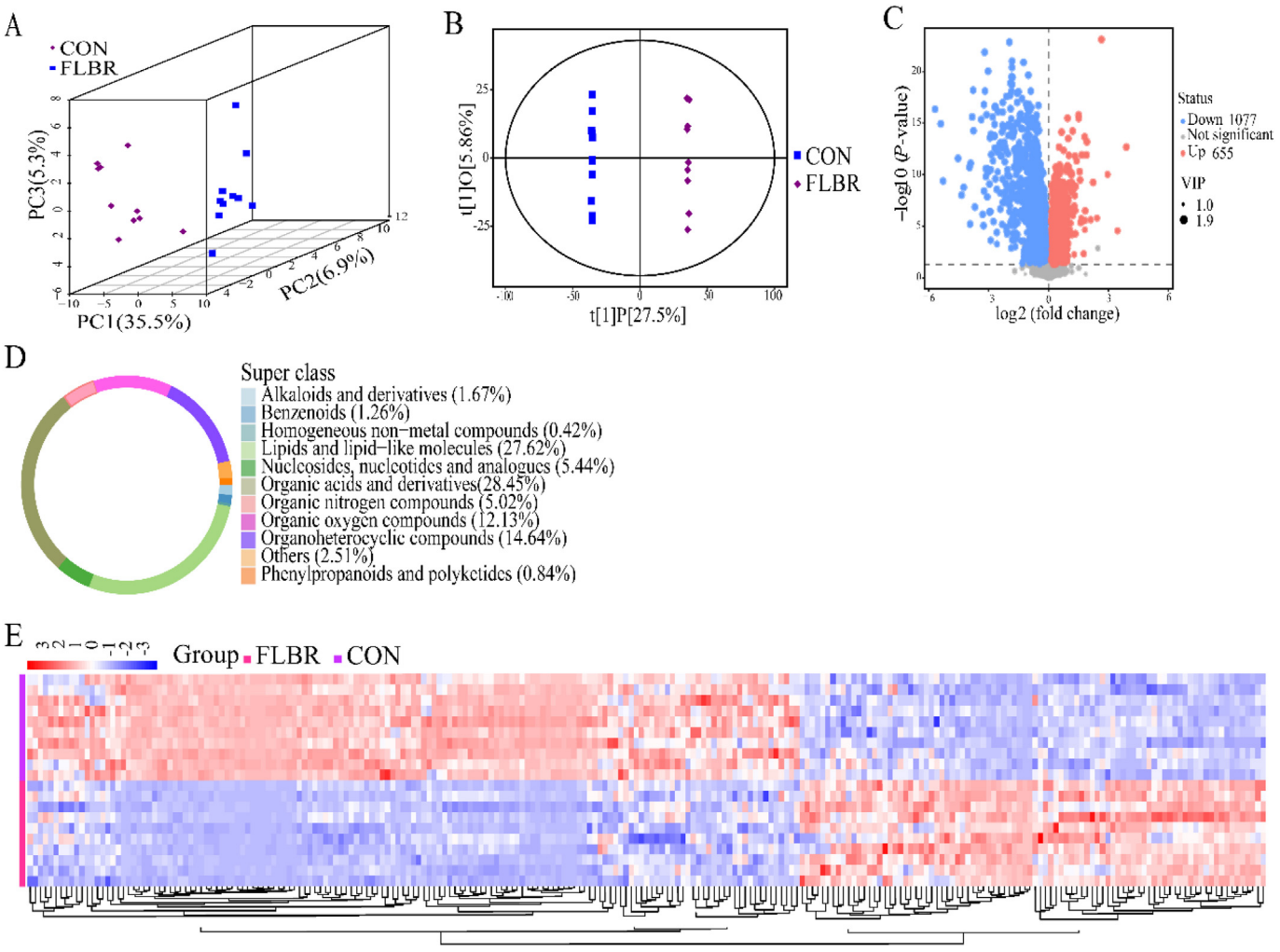


**Fig. 5. Effects of FLBR on metabolomic profiles of LT.** (A) PCA score plot 3D. (B) OPLS-DA score plot. (C) Volcano plot. (D) Super class and proportion of differential metabolites. (E) Heatmap of hierarchical clustering analysis. LBR = *L. barbarum* residues; FLBR = fermented *L. barbarum* residues; PCA = principal component analysis; OPLS-DA = orthogonal projections to latent structures-discriminant analysis; CON = basal diet without supplementation of LBR or FLBR; LT = longissimus thoracis.

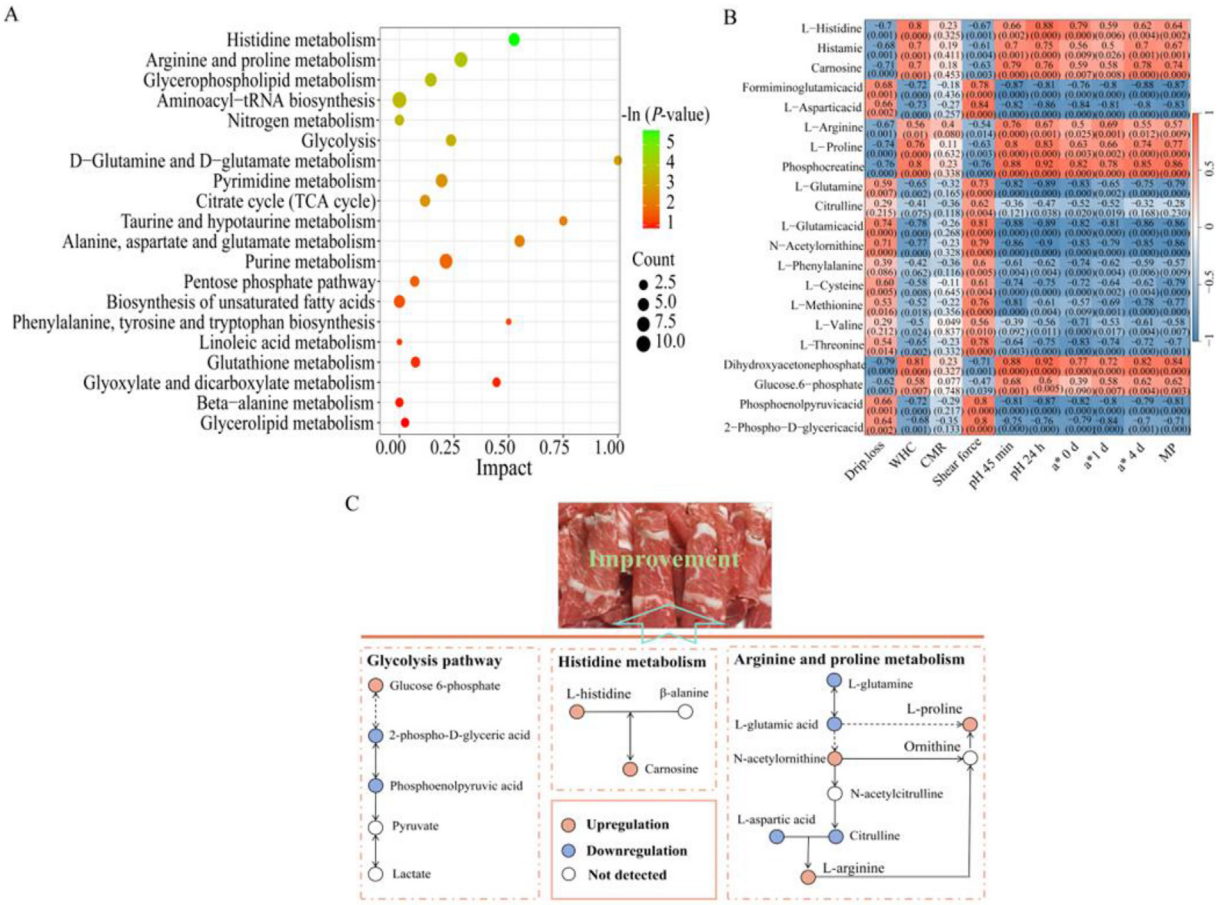


**Fig. 6. The LT metabolic pathway and metabolites analysis of lambs that accepted the FLBR diet compared with the CON diet.** (A) Enrichment of KEGG pathway; when the $P < 0.05$, a larger impact value means that FLBR treatment had a more significant effect on these metabolic pathways. (B) Pearson's correlation analysis of core metabolites with meat quality indicators and MP content. Red colors represent positive correlations, whereas blue colors represent negative correlations. Numerical values within a square represent Pearson's correlation coefficient and *P*-values. (C) Schematic diagram on FLBR improved the meat quality of lambs. LBR = *L. barbarum* residues; FLBR = fermented *L. barbarum* residues; CON = basal diet without supplementation of LBR or FLBR; KEGG = Kyoto Encyclopedia of Genes and Genomes; LT = longissimus thoracis; WHC = water holding capacity; CMR = cooked meat rate; MP = muscle protein.

*L. barbarum* polysaccharides can increase the relative abundances of rumen *Ruminococcus albus*, *Ruminococcus flavefaciens* and *Butyrivibrio fibrisolvens*, facilitating the breakdown of non-structural carbohydrates into water-soluble sugars (Li et al., 2018). The acetate and butyrate, the major products of carbohydrates fermentation in the rumen, are essential energy sources for various tissues, and key substrates for lipid biosynthesis (Laarman et al., 2012). Our findings reveal that lambs in FLBR group have a higher degradation of NDF and ADF, potentially providing an available carbon source for acetate production by rumen microorganisms. Propionate, another product of rumen fermentation, is rapidly absorbed by the rumen papillae and converted into glucose through gluconeogenesis, serving as a vital energy source for lambs (Amin and Mao, 2020). As a result, the levels of rumen propionate and serum glucose were elevated in the FLBR group, reflecting enhanced gluconeogenesis. Rumen microorganisms have been shown to ferment dietary amino acids or proteins into isobutyrate and isovalerate, which can reduce the efficiency of dietary protein utilization (Uushona et al., 2023). The lower levels of isobutyrate and isovalerate in FLBR group indicate that a greater amount of true protein in the feed is retained in the rumen, possibly improving protein utilization in the small intestine (McDonald et al., 2011). The higher levels of TP and lower level of UN in the FLBR group may directly reflect higher nitrogen utilization in these lambs. Plant polyphenols have been reported to inhibit ruminal lipolysis by encapsulating lipids within protein-phenol complexes, thereby reducing the substrate available for lipolytic enzymes (Vasta et al., 2019). Additionally, dietary polyphenols supplementation has been shown to inhibit biohydrogenation of unsaturated fatty acids (UFAs) by decreasing the relative abundance of *Anaerovibrio lipolytica* in the rumen of dairy ewes, thus slowing dietary lipid lipolysis (Mannelli et al., 2018). Consequently, the increased polyphenols content in the FLBR group may facilitate the flow of available UFAs to the duodenum, enhancing fat digestion. In summary, FLBR supplementation may increase the supply of protein, glucose and lipids to lambs by modulating rumen fermentation, supporting overall growth of lambs.

### 4.2. Transcriptomic profiling of LT and IMF tissues

Improving protein biosynthesis promotes skeletal muscle development, which directly influences the growth performance of lambs. With respect to protein metabolism in LT tissues, 9 DEGs (FLBR vs CON) encoding ribosomal protein were found to be significantly correlated with MP content. Ribosomes are constituted of two subunits, each containing its own assembly of many proteins and rRNA, and their common function is to perform protein biosynthesis in all living organisms. Previous studies have

shown that *RPL23A* enhanced milk proteins synthesis in dairy cattle through the transcription factors EGR1 and SP8 (Li et al., 2019). Conversely, lower expression of several ribosomal protein-encoding genes (*LOC101102122*, *LOC101114033*, *RPLP1* and *RPL3*) has been associated with proteolytic degradation of lambs, potentially contributing to reduced feed efficiency (Alba et al., 2018). Therefore, the higher levels of *RPL10A, RPL36AL, RPL9, RPL13* and *RPL6* in the FLBR lambs may promote protein anabolism, although their roles in muscle protein synthesis require in-depth validation. After FLBR supplementation, the increased protein supply in the small intestine may result from the reduced branched-chain fatty acids in rumen, a change that could be associated with the upregulation of these five ribosomal protein genes. Ribosomal proteins also exhibit the ribosome-independent functions. For instance, *RPL6* interacts directly with H2A histone and is rapidly recruited to sites of DNA damage to facilitate repair (Yang et al., 2018). It has been revealed that *RPL17* increased cancer risk in cell and mouse models by stimulating extracellular-regulated protein kinase and NIMA-related kinase 2/beta-catenin signaling axis (Ko et al., 2022). The higher level of *RPL6* and lower level of *RPL17* in the FLBR group may therefore support both growth and health in lambs. In comparison to the LBR diet, FLBR diet-triggered DEGs were functionally associated with immune response, amino acid metabolism, fatty acid metabolism and xenobiotics metabolism in lambs. The synergy of *C9*, *C8B* and *C7* in the complement system played an important role in innate immune defense by assembling membrane attack complexes and rapidly causing the destruction of target cells (Mu et al., 2023). Additionally, the antithrombin III encoded by *SERPINC1* exhibits anti-inflammatory effects through the enhancement of prostaglandin I2 (Wang et al., 2015), while *ITGB2* gene in swine mediates inflammatory responses through leukocyte trafficking, macrophage activation, and phagocytosis (Namous et al., 2023). The genes *ACACA*, *FASN*, *ACSS2*, *ELOVL6*, *SCD*, *ACSL6* and *HSD17B12* were identified as key determinants in fatty acid biosynthesis (Fig. 4E). Furthermore, the upregulated genes *PAH* and *TAT* serve as key regulatory nodes in phenylalanine and tyrosine metabolism. The glucuronidation process, catalyzed by *UGT2B7*, plays crucial roles in endobiotic homeostasis, xenobiotics metabolism and metabolic defense, particularly in the detoxification of exogenous compounds (Yuan et al., 2015). Notably, some novel DEGs involved in xenobiotic metabolism, such as *LOC101117764*, *LOC101119393*, *LOC114108597* and *LOC101111965*, were found to be highly interactive, although their precise functions remain unclear. In summary, a FLBR diet has been shown to improve the growth performance of lambs by modulating multiple metabolic pathways, distinguishing it from the effects observed with the CON or LBR diets.

Transcriptomic analysis of IMF offers a logical and insightful approach for identifying mechanisms that influence the growth performance of lambs. With respect to lipid metabolism in IMF tissues, 10 DEGs (FLBR vs CON), including *LEP*, *ACACA*, *FASN*, *CPT2*, *HSD17B12*, *ELOVL6*, *ACSL1*, *ACSL6*, *LPL* and *ACAT2*, were discovered to have significant correlations with the IMF content. Compared to the LBR diet, the genes *ACSL1*, *FADS1*, *SCD*, *ACSL6*, *ELOVL6*, *HACD2*, *ACAT2*, *FADS1*, *ELOVL3*, *FASN*, *ACACA*, *LPL* and *LEP* in lambs fed the FLBR diet were significantly upregulated and exhibited high interactivity, suggesting that FLBR diet exerts a more pronounced impact on lipid biosynthesis. *FASD1* synthesized polyunsaturated fatty acids with different saturations by introducing double bonds to defined carbons of the fatty acyl chain (Dervishi et al., 2019). As a rate-limiting enzyme in the monounsaturated fatty acid synthesis, *SCD* is implicated in IMF deposition through its role in the differentiation of precursor adipocytes (Zhang et al., 2019). The excessive accumulation of lipids stimulates the *LEP* expression, which subsequently regulates appetite and maintains energy homeostasis within the organism (Zhang et al., 2005). It has been documented that *ACACA* is mainly responsible for converting acetyl-CoA to malonyl-CoA, a precursor synthesizing fatty acids (Wang et al., 2022). It is one of rate-limiting enzymes participating in lipid biosynthesis. The *ACACA* played key roles in shaping IMF phenotype of cattle skeletal muscle (Jager et al., 2013). *FASN* is a core activator of fatty acid synthesis (palmitate, C16:0) de novo, facilitating substantial lipid storage in adipose tissues (Fan et al., 2019). Our study found these 5 genes were significantly up-regulated by the FLBR diet. *CPT2* serves as a critical rate-limiting enzyme for the $\beta$-oxidation of long-chain fatty acids (LCFAs), converting fatty acids into energy and acetyl-CoA (Bonnefont et al., 2004). The increased acetyl-CoA levels in the presence of FLBR may provide the initial substrate necessary for IMF formation. Beyond its role in stearate (C18:0) synthesis, 7 members (*ELOVL1-7*) from *ELOVL* family along with *HSD17B12* were considered key candidate genes involved in the elongation of LCFAs and regulation of fatty acid composition (Bakhtiarizadeh and Alamouti, 2020). The *ACSL*, with its 5 isoforms (*ACSL*1, -3, -4, -5, and -6), catalyzes the thioesterification of 12 to 20 carbons-FAs with CoA to generate various fatty acyl-CoAs, which are then involved in multiple metabolic fates such as membrane synthesis, $\beta$-oxidation, FAs-desaturation and elongation, and the synthesis of TG, phospholipids, retinal esters and cholesterol esters (Grevengoed et al., 2014). The data indicated that *ACSL1*, *ACSL6* and *ELOVL6* were highly expressed in the FLBR group. The TG in lipoprotein particles is decomposed into 2-monoacylglycerol and free fatty acids under *LPL* actions, which can then provide energy for other tissues or be re-synthesized into TG (Huang et al., 2018). The *ACAT* family at the endoplasmic reticulum are composed of two isoforms (*ACAT1-2*), and their primary function is to catalyze the esterification of free cholesterol and LCFAs or fatty acyl-CoA to produce cholesterol esters (Shibuy et al., 2015). Our data revealed that these genes were differentially expressed due to the FLBR supplementation, indicating FLBR exerted a significant role in IMF deposition. Although the exact mechanisms by which FLBR influences these genes are yet unclear. Taken together, the inclusion of FLBR in the feed increased fatty acid anabolism, thus providing additional energy required for maintenance and fattening.

### 4.3. Metabolomic profiling of LT tissue

Color is a visual dominant of meat freshness, strongly influencing consumers' sensory acceptance and purchase decisions, and is directly determined by the myoglobin content and its redox state (Ramanathan et al., 2020). Carnosine, a bioactive dipeptide composed of L-histidine and β-alanine, has been found to decrease *b** value and high-iron myoglobin content in meat. Furthermore, it preserves meat color by preventing meat lipid and protein oxidation through its roles in free radicals scavenging, metals chelation and hydrogen donation (Yeh et al., 2020). Previous research has confirmed that dietary supplementation with *L. barbarum* polysaccharides can enhance antioxidant activity in broiler chicken, leading to a stable meat color (Long et al., 2020). Similarly, tea polysaccharides have been found to stimulate Mb synthesis and fat deposition in muscle, thereby causing a greater color *a** value (Li et al., 2020). Polyphenols also offer antioxidant protection for meat pigments and lipids, resulting in a higher color *a** value when incorporated into the diets of goats (Giller et al., 2021). Currently, FLBR and its extracts have displayed exceptional antioxidant capacities both in vivo and in vitro, as indicated in Table S1. It is therefore hypothesized that FLBR significantly increased postmortem *a** value at 0, 1 and 4 d due to the antioxidant activity of the carnosine, polysaccharide and polyphenols. Rapid lactic acid accumulation in the glycolysis pathway has been reported to modify the intermolecular forces, spatial structure and water solubility of meat myoglobin, myosin and actin. This leads to a serious

deterioration in post-mortem color, tenderness and WHC (Zuo et al., 2016). In this study, the higher level of muscle glycogen and lower concentrations of 2-p-D-ga and PEP in glycolysis pathway, suggest that FLBR supplementation may delay post-mortem glycolysis reaction and pH decline, ultimately improving meat quality. Previous studies have shown that carnosine can improve pH value and WHC, while reducing shear force in chicken meat (Suwanvichanee et al., 2022) and pork (Yu et al., 2023) by delaying post-mortem glycolysis. Based on these findings, it is estimated that FLBR possibly improves meat quality by modulating carnosine content and the glycolysis pathway.

The primary function of aminoacyl-tRNA is to transport free amino acids into ribosomes for protein synthesis, a process catalyzed by aminoacyl-tRNA synthetases (Bryson et al., 2017). In this study, the levels of 7 free amino acids, including L-phenylalanine, L-valine and L-threonine in the Aminoacyl-tRNA pathway, were found to be lower compared to the CON. This suggests that these amino acids are predominantly utilized for protein synthesis. Conversely, the increased levels of glycogen-producing amino acid, such as L-histidine, L-arginine and L-proline, indicate a potential decrease in their participation in gluconeogenesis, which may lead to a higher amino acid utilization efficiency in lambs supplemented with FLBR (Ijaz et al., 2022). Previous studies have underscored the beneficial roles of L-arginine and L-proline in protein synthesis and oxidants scavenging in animals (Wang et al., 2021). For example, *M. officinalis* polysaccharides have been shown to enhance the activities of antioxidant enzymes by stimulating arginine and proline synthesis, thereby mitigating oxidative damage in meat (Huang et al., 2021). This finding aligns with our results that FLBR supplementation increases SOD activity. Moreover, Ge et al. (2023) reported that elevated muscle arginine were associated with reduced color $L^*$ and $b^*$ values, as well as decreased shear force. These results support the metabolism of arginine and proline as a key pathway in meat quality improvement.

## 5. Conclusion

The enhanced growth performance of lambs observed in lambs with the addition of 5.0% (w/w) FLBR may be associated with the alterations in rumen fermentation patterns and nutrient digestibility. Some core DEGs in LT tissues, such as *RPL10A*, *RPL6*, *C9*, *SERPINC1*, *ITGB2*, *PAH* and *UGT2B7*, revealed the importance of protein biosynthesis, immune response, amino acids metabolism and xenobiotics metabolism in the growth and development of FLBR lambs. The genes like *ACACA*, *FASN*, *ELOVL6* and *ACSL1* are regarded as the potential regulatory sites for lipid biosynthesis in IMF tissue of the FLBR lambs. These genes preliminarily showed the molecular mechanism of FLBR in improving the growth performance of lambs. The metabolic pathways affected by the FLBR diet may contribute to the improvement in meat quality, especially those involved in Histidine metabolism, Arginine and proline metabolism, and Glycolysis metabolism. These results may provide novel insights into the efficient roles of FLBR in improving the growth performance and meat quality of lambs, and its regulatory mechanisms. Future trials will involve the higher dietary inclusion levels, a larger group of lambs, and different breeds to validate the putative biomarkers identified in this study.

## Credit Author Statement

**Jiale Liao:** Writing – original draft, Visualization, Software, Methodology, Investigation, Formal analysis, Data curation, Conceptualization. **Wencan Ke:** Writing – review & editing, Visualization, Supervision, Software. **Bing Wang:** Writing – review & editing, Software. **Min Du:** Writing – review & editing, Visualization. **Qiang Lu:** Writing – review & editing, Supervision, Software. **Yajun Zhang:** Writing – review & editing, Visualization, Software. **Guijie Zhang:** Visualization, Validation, Supervision, Resources, Project administration, Methodology, Investigation, Funding acquisition.

## Data availability statement

Correspondent authors upon reasonable requests will provide raw data supporting the findings of this study. The raw unprocessed sequence data of longissimus thoracis and intramuscular fat tissues are available at NCBI SRA database with a BioProject accession code (PRJNA941128).

## Declaration of competing interest

We declare that we have no financial and personal relationships with other people or organizations that can inappropriately influence our work, and there is no professional or other personal interest of any nature or kind in any product, service and/or company that could be construed as influencing the content of this paper.

## Acknowledgements

We thank our colleagues for their help in collecting the data. This work obtained financial and technical supports from the National Key Research and Development Program of China (2022YFD1300905), Top Discipline Construction Project of Pratacultural Science (NXYLXK2017A01), and the Key Research and Development Program of Ningxia Hui Autonomous Region (2021BEF02020and 2021BBF02034).

## Appendix A. Supplementary data

Supplementary data to this article can be found online at https://doi.org/10.1016/j.aninu.2024.11.002.

## References

Amin AB, Mao SY. Influence of yeast on rumen fermentation, growth performance and quality of products in ruminants: a review. Anim Nutr 2020;7:31–41.
Adorno MAT, Hirasawa JS, Varesche MBA. Development and validation of two methods to quantify volatile acids (C2-C6) by GC/FID: headspace (automatic and manual) and liquid-liquid extraction (LLE). Am J Anal Chem 2014;5:406–14.
Alba S, Francisco JG, Erminio T, Luigi L, Javier F, Sonia A. Liver transcriptomic and plasma metabolomic profiles of fattening lambs are modified by feed restriction during the suckling period. J Anim Sci 2018;96:1495–507.
AOAC. Official methods of analysis. 18th ed. Gaithersburg, MD, USA: AOAC International; 2006.
AOAC. Official Methods of Analysis. 17th ed. Gaithersburg, MD, USA: AOAC International; 2000.
Bakhtiarizadeh MR, Alamouti AA. RNA-Seq based genetic variant discovery provides new insights into controlling fat deposition in the tail of lambs. Sci Rep-UK 2020;10:13525.
Biffin TE, Smith MA, Bush RD, Morris S, Hopkins DL. The effect of whole carcase medium voltage electrical stimulation, tenderstretching and longissimus infusion with actinidin on alpaca meat quality. Meat Sci 2020;164:108107.
Bonnefont JP, Djouadi F, Prip-Buus C, Gobin S, Munnich A, Bastin J. Carnitine palmitoyltransferases 1 and 2: biochemical, molecular and medical aspects. Mol Aspect Med 2004;25:495–520.
Bryson DI, Fan C, Guo LT, Miller C, Soll D, Liu DR. Continuous directed evolution of aminoacyl-tRNA synthetases. Nat Chem Biol 2017;13:12–23.
China National Standard. Determination of calcium in feeds. GB/T 6436-2018. Beijing: Standards Press of China; 2018a.
China National Standard. Determination of phosphorus in feeds-spectrophotometry. GB/T 6437-2018. Beijing: Standards Press of China; 2018b.
China National Standard. Determination of neutral detergent fiber (NDF) in feeds. GB/T 20806-2022. Beijing: Standards Press of China; 2022.
Cui YY, Peng S, Deng D, Yu M, Tian ZM, Song M, et al. Solid-state fermentation improves the quality of chrysanthemum waste as an alternative feed ingredient. J Environ Manag 2023;330:117060.

Dai CH, Ma HL, He RH, Huang LR, Zhu SY, Ding QZ, et al. Improvement of nutritional value and bioactivity of soybean meal by solid-state fermentation with *Bacillus subtilis*. LWT-food Sci Technol 2017;86:1–7.
Debi MR, Wichert BA, Wolf P, Liesegang A. Effect of a two-step fermentation method with rumen liquor on protein quality of wheat bran and rice bran to use as poultry feed. Heliyon 2022;8(12):e11921.
Dervishi E, González-Calvo L, Blanco M, Joy M, Sarto P, Martin-Hernandez R, et al. Gene expression and fatty acid profiling in longissimus thoracis muscle, subcutaneous fat, and liver of light lambs in response to concentrate or alfalfa grazing. Front Genet 2019;10:1070.
Fan YX, Ren CF, Meng FX, Deng KP, Zhang GM, Wang F. Effects of algae supplementation in high-energy dietary on fatty acid composition and the expression of genes involved in lipid metabolism in Hu lambs managed under intensive finishing system. Meat Sci 2019;157:107872.
Gao XG, Wang ZY, Miao J, Xie L, Dai Y, Li XM, et al. Influence of different production strategies on the stability of color, oxygen consumption and metmyoglobin reducing activity of meat from Ningxia *Tan lambs*. Meat Sci 2014;96:769–74.
Ge Y, Kai G, Li Z, Chen Y, Wang L, Qi XL, et al. HPLC-QTRAP-MS-based metabolomics approach investigates the formation mechanisms of meat quality and flavor of Beijing You chicken. Food Chem X 2023;17:100550.
Giller K, Sinz S, Messadene-Chelali J, Marquardt S. Maternal and direct dietary polyphenol supplementation affect growth, carcass and meat quality of lambs and goats. Animal 2021;15:100333.
Grevengoed TJ, Klett EL, Coleman RA. Acyl-CoA metabolism and partitioning. Annu Rev Nutr 2014;34:1–30.
Huang HL, Zhang Y, Cao MY, Xue LY, Shen WL. Effects of fasting on the activities and mRNA expression levels of lipoprotein lipase (LPL), hormone-sensitive lipase (HSL) and fatty acid synthetase (FAS) in spotted seabass Lateolabrax maculatus. Fish Physiol Biochem 2018;44:387–400.
Huang SC, Cao QQ, Cao YB, Yang YR, Xu TT, Yue K, et al. *Morinda officinalis* polysaccharides improve meat quality by reducing oxidative damage in chickens suffering from tibial dyschondroplasia. Food Chem 2021;344:128688.
Ijaz M, Zhang DQ, Hou CL, Mahmood M, Hussain Z, Zheng XC, et al. Changes in postmortem metabolites profile of atypical and typical DFD beef. Meat Sci 2022;193:108922.
Jager ND, Hudson NJ, Reverter A, Barnard R, Café LM, Greenwood PL, et al. Gene expression phenotypes for lipid metabolism and intramuscular fat in skeletal muscle of cattle. J Anim Sci 2013;91:1112–28.
Ko MJ, Seo YR, Seo D, Park SY, Seo JH, Jeon EH, et al. RPL17 promotes colorectal cancer proliferation and stemness through ERK and NEK2/β-catenin Signaling Pathways. J Cancer 2022;13:2570–83.
Laarman AH, Ruiz-Sanchez AL, Sugino T, Guan LL, Oba M. Effects of feeding a calf starter on molecular adaptations in the ruminal epithelium and liver of Holstein dairy calves. J Dairy Sci 2012;95(5):2585–94.
Licitra G, Hernandez TM, Van Soest PJ. Standardization of procedures for nitrogen fractionation of ruminant feeds. Anim Feed Sci Technol 1996;57:347–58.
Li X, Chen S, Zhao ZT, Zhao M, Han Y, Ye XM, et al. Effects of polysaccharides from Yingshan Yunwu tea on meat quality, immune status and intestinal microflora in chickens. Int J Biol Macromol 2020;155(15):61–70.
Li Y, Han B, Liu L, Zhao F, Liang W, Jiang J, et al. Genetic association of *DDIT3, RPL23A, SESN2* and *NR4A1* genes with milk yield and composition in dairy cattle. Anim Genet 2019;50:123–35.
Li ZJ, Bai HX, Zheng LX, Jiang H, Cui HY, Cao YC, et al. Bioactive polysaccharides and oligosaccharides as possible feed additives to manipulate rumen fermentation in Rusitec fermenters. Int J Biol Macromol 2018;109:1088–94.
Long F, Zhang ZY, Chen JY, Yang S, Tian Y, Mei CG, et al. The role of BBS2 in regulating adipogenesis and the association of its sequence variants with meat quality in Qinchuan cattle. Genomics 2022;114:110416.
Long LN, Kang BJ, Jiang Q, Chen JS. Effects of dietary *Lycium barbarum* polysaccharides on growth performance, digestive enzyme activities, antioxidant status, and immunity of broiler chickens. Poultry Sci 2020;99:744–51.
Lopez-Carlos MA, Ramírez RG, Aguilera-Soto JI, Arechiga CF, Rodríguez H. Size and shape analyses in hair sheep ram lambs and its relationships with growth performance. Livest Sci 2010;131:203–11.
Mannelli F, Cappucci A, Pini F, Pastorelli R, Decorosi F, Giovannetti L, et al. Effect of different types of olive oil pomace dietary supplementation on the rumen microbial community profile in Comisana ewes. Sci Rep-UK 2018;8:8455.
Ma R, Zhang X, Thakur K, Zhang J, Wei ZJ. Research progress of *Lycium barbarum* L. as functional food:phytochemical composition and health benefits. Curr Opin Food Sci 2022;47:100871.
Mcdonald P, Edwards RA, Greenhalgh JFD, Morgan CA, Sinclair LA, Wilkinson RG. Animal nutrition. 7th ed. Harlow, England: Pearson; 2011.
Menchetti L, Brecchia G, Branciari R, Barbato O, Fioretti B, Codini M, et al. The effect of Goji berries (Lycium barbarum) dietary supplementation on rabbit meat quality. Meat Sci 2020;161:108018.
Mu LL, Qiu L, Li JD, Bai H, Lei Y, Zeng QL, et al. C9 regulates the complement-mediated cell lysis in association with CD59 to resist bacterial infection in a primary animal. Int J Biol Macromol 2023;239:124317.
Namous H, Strillacci MG, Braz CU, Shanmuganayagam D, Krueger C, Peppas A, et al. ITGB2 is a central hub-gene associated with inflammation and early fibro-atheroma development in a swine model of atherosclerosis. Atherosclerosis 2023;54:30–41.
Ramanathan R, Suman SP, Faustman C. Biomolecular interactions governing fresh meat color in post-mortem skeletal muscle: a review. J Agric Food Chem 2020;68:12779–87.
Shibuy Y, Chang CCY, Chang TY. ACAT1/SOAT1 as a therapeutic target for Alzheimer's disease. Future Med Chem 2015;7.
Suwanvichanee C, Sinpru P, Promkhun K, Kubota S, Riou C, Molee W, et al. Effects of β-alanine and L-histidine supplementation on carnosine contents in and quality and secondary structure of proteins in slow-growing Korat chicken meat. Poultry Sci 2022;101:101776.
Tan XH, Sun ZZ, Ye CX. Dietary Lycium barbarum extract administration improved growth, meat quality and lipid metabolism in hybrid grouper (Epinephelus lanceolatus ♂ × E. fuscoguttatus ♀) fed high lipid diets. Aquaculture 2019;504:190–8.
Uushona T, Chikwanha OC, Katiyatiya CLF, Strydom PE, Mapiye C. Substitution effects of *Acacia mearnsii* leaf-meal for *Triticum aestivum* bran on nutrient digestibility, rumen fermentation and nitrogen retention in lambs. Small Rumin Res 2023;221:106948.
Vasta V, Daghio M, Cappucci A, Buccioni A, Serra A, Viti C, et al. Plant polyphenols and rumen microbiota responsible for fatty acid biohydrogenation, fiber digestion, and methane emission: experimental evidence and methodological approaches. J Dairy Sci 2019;102:3781–804.
Wang F, Zhang GY, Lu ZY, Geurts AM, Usa K, Jacob HJ, et al. Antithrombin III/SerpinC1 insufficiency exacerbates renal ischemia/reperfusion injury. Kidney Int 2015;88:796–803.
Wang Q, Cao H, Su XH, Liu WJ. Identification of key miRNAs regulating fat metabolism based on RNA-seq from fat-tailed lambs and F2 of wild Argali. Gene 2022;834:146660.
Wang QC, Xu Z, Ai QH. Arginine metabolism and its functions in growth, nutrient utilization, and immunonutrition of fish. Anim Nutr 2021;7:716–27.
Wang X, Xie HJ, Liu F, Wang YH. Production performance, immunity, and heat stress resistance in Jersey cattle fed a concentrate fermented with probiotics in the presence of a Chinese herbal combination. Anim Feed Sci Technol 2017;228:59–65.
Yang CZ, Zang WC, Ji YP, Li TT, Yang YF, Zheng XF. Ribosomal protein L6 (RPL6) is recruited to DNA damage sites in a poly (ADP-ribose) polymerase– dependent manner and regulates the DNA damage response. J Biol Chem 2018;294:2827–5664.
Yang ZH, Hou YR, Zhang M, Hou PX, Liu C, Dou L, et al. Unraveling proteome changes of Sunit lamb meat in different feeding regimes and its relationship to flavor analyzed by TMT-labeled quantitative proteomic. Food Chem 2024;437:137657.
Yeh H, Line JE, JR AH, Gao Y, Zhuang H. Bacterial community assessed by utilization of single carbon sources in broiler ground meat after treatment with an antioxidant, carnosine, and cold plasma. J Food Protect 2020;83:1967–73.
Yuan L, Qian S, Xiao Y, Sun H, Zeng S. Homo- and hetero-dimerization of human UDP-glucuronosyltransferase 2B7 (UGT2B7) wild type and its allelic variants affect zidovudine glucuronidation activity. Biochem Pharmacol 2015;95:58–70.
Yu T, Tian X, Li D, He Y, Yang P, Cheng Y, et al. Transcriptome, proteome and metabolome analysis provide insights on fat deposition and meat quality in pig. Food Res Int 2023;116:112550.
Zhan HW, Xiong YC, Wang ZC, Dong WJ, Zhou QH, Xie SS, et al. Integrative analysis of transcriptomic and metabolomic profiles reveal the complex molecular regulatory network of meat quality in Enshi black pigs. Meat Sci 2022;183:108642.
Zhang BY, Sun ZQ, Yu Z, Li HH, Luo HL, Wang B. Transcriptome and targeted metabolome analysis provide insights into bile acids' new roles and mechanisms on fat deposition and meat quality in lamb. Food Res Int 2022;162:111941.
Zhang FM, Chen YY, Heiman M, DiMarchi R. Leptin: structure, function and biology. Vitam Horm 2005;71:345–72.
Zuo HX, Han L, Yu QL, Niu KL, Zhao SN, Shi HM. Proteome changes on water-holding capacity of yak *longissimus lumborum* during postmortem aging. Meat Sci 2016;121:409–19.
Zhang YF, Zhang JJ, Gong HF, Cui LL, Zhang WC, Ma JW, et al. Genetic correlation of fatty acid composition with growth, carcass, fat deposition and meat quality traits based on GWAS data in six pig populations. Meat Sci 2019;150:47–55.